

Supplementary Materials for

A clinically translatable, irreversibly attenuated *Salmonella* strain as a next-generation adjuvant for checkpoint immunotherapy

Dinh-Huy Nguyen *et al.*

Corresponding authors:

Jung-Joon Min (jjmin@jnu.ac.kr) and Yeongjin Hong (yjhong@jnu.ac.kr)

This PDF file includes:

Materials and Methods

Figure S1 to S24

Table S1 to S5

Materials and Methods

NO colorimetric assay

The tumor-derived nitric oxide (NO) levels were measured indirectly by determining nitrite + nitrate concentrations with the Nitric Oxide Colorimetric Assay Kit (Abcam, Cat # ab65328, UK) following the manufacturer's protocol. Three days after bacterial inoculation, tumors were excised, minced, and homogenized on ice in lysis buffer (1 g tissue: 4 mL buffer, w/v) containing a protease-inhibitor cocktail. After a 1-hour incubation on ice, the homogenates were centrifuged at $10,000 \times g$ for 10 min at 4°C ; the resulting supernatants were collected, and protein concentrations were measured with a BCA assay. To improve NO stability, the supernatants were passed through a 10 kDa molecular-weight-cut-off filter (Abcam) and stored at -80°C . For the assay, each sample and its corresponding standards were incubated with nitrate reductase and its co-factor for 1 h at room temperature to convert nitrate to nitrite. The Griess-reaction reagents were then added, allowing nitrite to form a purple azo-chromophore; the color was allowed to develop for 10 min. Absorbance was read at 540 nm, providing a detection limit of $1 \mu\text{M}$ based on a linear calibration curve. NO concentrations were finally expressed as $\mu\text{M}/\text{mg}$ of total protein.

Measurement of cytokine levels

The levels of the pro-inflammatory cytokines IL-4, IL-6, IL-10, IL-1 β , TNF- α , and IFN- γ were quantified by enzyme-linked immunosorbent assay (ELISA) using commercial kits (ABclonal Technology, China) according to the manufacturers' protocols.

Bacterial biodistribution in tumor-bearing mice

Bioluminescent *SL Δ ppGpp-lux* and *CNC018-lux* bacteria (4×10^7 CFU) in 100 μL of PBS were injected i.v. into CT26 s.c. tumor-bearing mice. Bioluminescence signals were imaged in the whole body on days 1, 3, and 5 after bacterial treatment using an IVIS Lumina system (PerkinElmer, USA). Bioluminescent signals were quantified within regions of interest as maximum photons per second (p/s) units.

To evaluate *in vivo* bacterial distribution, *SL Δ ppGpp* (2×10^7 CFU) was administrated via tail-vein injection. At the indicated time points (1, 3, and 5 days), tumors and normal organs were

harvested, weighed, and subjected to mechanical homogenization in PBS (3:1 ratio of volume (mL) per tissue gram (g)) using an IKAT10 Basic ULTRA-TURRAX homogenizer (IKA Dispersers, Germany). Tissue homogenates were serially diluted 10-fold in sterile PBS and plated onto LB agar. Following an overnight incubation at 37 °C, the resulting colonies were enumerated. Bacterial burdens were subsequently normalized and reported as CFU per gram of tissue or per milliliter of blood.

Antibiotic susceptibility profile of CNC018 in tumor-bearing mice

To investigate the antibiotic-mediated clearance of CNC018, CT26-tumor-bearing mice (tumor volume ~100 - 120 mm³) were intravenously challenged with the bacteria (2×10^7 CFU) on day 0. Oral ciprofloxacin therapy was initiated on day 5 with an initial dose of 60 mg/kg, followed by subsequent daily administrations of 100 mg/kg. To determine the rate of bacterial elimination, tumor tissues and major host organs were harvested on days 4, 7, 14, and 21 for quantitative colony counting. The effectiveness of the antibiotic regimen was assessed by comparing the residual bacterial burden across these time points.

DC maturation assay

Primary bone marrow cells were isolated from the tibiae and femurs of BALB/c mice. These cells were maintained in RPMI-1640 (Gibco-BRL, USA) containing 10% FBS, and 1% penicillin-streptomycin and supplemented with murine recombinant GM-CSF (20 ng/mL) and IL-4 (10 ng/mL) (both from R&D Systems). Fresh cytokine-enriched medium was replenished by half-volume exchange on days 2 and 4. On the sixth day of culture, cells were harvested using mechanical scraping and prepared in PBS. For purification, the cells were labeled with CD11c-conjugated magnetic beads (Miltenyi Biotec, USA) for 30 min, and CD11c⁺ immature dendritic cells (imDCs) were isolated using a MACS Separator (Miltenyi Biotec, Germany) following the provided guidelines. To generate mature DCs (mDCs), the imDCs were further incubated at 37 °C for an additional 48 h.

To evaluate DC activation, CT26 cells (5×10^5) were first cultured overnight in 6-well plates using 10% FBS-DMEM and then exposed to CNC018 (5×10^5 CFU) for 18 h. Subsequently, either the CNC018-primed CT26 cells (4×10^5) or their conditioned media were retrieved and co-incubated with imDCs (2×10^5) for 24 h. In neutralizing experiments, CNC018-treated CT26

cells were pre-incubated with 10 µg/mL of anti-HMGB1 or anti-CALR antibodies (Abcam, UK) for 5 h before being introduced to the imDCs. The phenotypic maturation of DCs was subsequently characterized through flow cytometric analysis of surface marker expression.

Treatment of neutralizing antibody in tumor-bearing mice

For the systemic depletion of CD8⁺ T cells, mice were administered 200 µg of an anti-mouse CD8 monoclonal antibody (Bio X Cell, USA) via intraperitoneal (i.p.) injection. This regimen (approximately 10 mg/kg) commenced 24 h prior to bacterial inoculation and was maintained twice weekly for a total of five doses throughout the experimental timeline. For DAMP sequestration studies, either a rabbit anti-HMGB1 antibody (20 µg/mouse; Arigo, Taiwan) or a rabbit anti-CALR antibody (25 µg/mouse; Abcam, UK), diluted in 200 µL of PBS, was delivered i.p. following the same administration frequency and timing established for the T-cell depletion groups.

Characterization of tumor-associated immune populations

At 3 or 6 days post-bacterial administration, solid tumor masses, spleens, and TdLNs were excised and placed in 2 mL of chilled isolation medium (RPMI 1640 containing 5% FBS, 1% L-glutamine, 1% penicillin-streptomycin, and 10 mM HEPES). Following mechanical dissociation, tissue fragments were enzymatically digested using 1 mg/mL collagenase type IV and 50 µg/mL DNase I (both from Roche, Switzerland) for 20 - 30 min at 37 °C. Erythrocytes were eliminated by adding an equal volume of 1× RBC lysis buffer (BioLegend, USA) to the 2-mL cell suspension for 4 min at 37 °C. The resulting cell suspensions were passed through 100-µm and then 40-µm mesh filters (BD Falcon, USA). Before antibody labeling, cells were treated with Fc receptor blocking buffer (BioLegend, USA) for 10 min at room temperature. The leukocytes were then incubated on ice for 30 min with fluorophore-conjugated antibodies ([Table S3](#)) and quantified using flow cytometry.

To identify tumor-antigen-specific CD8⁺ T cells, TdLNs were collected on day 6 from mice in the PBS, CNC018, and *SLΔppGpp* treatment groups. These cells were simultaneously stained with an APC-labeled H-2Ld MuLV gp70 tetramer (SPSYVYHQF; MBL, USA) and a PE-labeled anti-CD8 monoclonal antibody (Ebioscience, USA) before flow cytometric evaluation.

Supplementary Information

Supplementary Figures

Figure S1. *In vivo* invasion of tumor-colonizing bacteria in CT26 tumors measured by gentamicin-protection assay.

Figure S2. Genetic stability and safety of CNC018 during serial passaging.

Figure S3. *In vivo* characterizations of CNC018.

Figure S4. Systemic toxicity of CNC018.

Figure S5. Systemic safety and long-term tolerability of CNC018.

Figure S6. Biosafety and antitumor effects of VNP20009 and CNC018.

Figure S7. Gating strategies of flow cytometry analysis.

Figure S8. CNC018-induced pro-inflammatory responses are mediated by the stimulation of multiple signaling pathways in the TME.

Figure S9. ScRNA-seq analysis of marker and cytokine transcript expression in CD3⁺ T cells infiltrating tumors.

Figure S10. DAMPs released from CNC018-induced dying tumor cells.

Figure S11. Photos of mice with CT26 tumors taken before and after treatment with CNC018 and anti-DAMP antibodies.

Figure S12. Generation of colon cancer PDX tumor model.

Figure S13. Tumor size and flow cytometry analysis of PDX tumors treated with CNC018.

Figure S14. CNC018 suppresses growth of primary and metastatic murine tumors.

Figure S15. CNC018 inhibits liver metastasis.

Figure S16. PD-L1 expression on cancer cell lines (CT26, MC38, 4T1, B16F10) *in vitro*.

Figure S17. CNC018 strongly potentiates the anti-tumor efficacy of ICB against CT26 tumors.

Figure S18. HMGB1 is required for the combination of CNC018 and α PD-L1 antibody to suppress tumors.

Figure S19. ScRNA-seq analysis of TLR4 and TLR5 mRNA expression in total cells from CT26 tumors.

Figure S20. Antitumor effect of CNC018 combined with anti-PD-L1 immunotherapy on tumor growth in knockout mice.

Figure S21. IFN- γ is required for the combination of CNC018 and α PD-L1 antibody to suppress tumors.

Figure S22. Tumor suppression by the synergistic combination of CNC018 and α PD-L1 in MC38 tumor-bearing mice.

Figure S23. Antitumor effects of 5-FU and CNC018 strain in combination with anti-PD-L1 immunotherapy.

Figure S24. Tumor suppression by the synergistic combination of CNC018 and α PD-L1 in MC38 dual tumor-bearing mice treated by intratumoral injection.

Supplementary tables

Table S1. Strains and plasmids are used in this study.

Table S2. Oligonucleotide primers of PCR amplification for bacterial genotyping.

Table S3. Antibodies used in this study.

Table S4. Xenograft pathological subtype changes of patient colon cancer.

Table S5. CDI value of CNC018 plus ICB blockade in CT26 and MC38 tumor models.

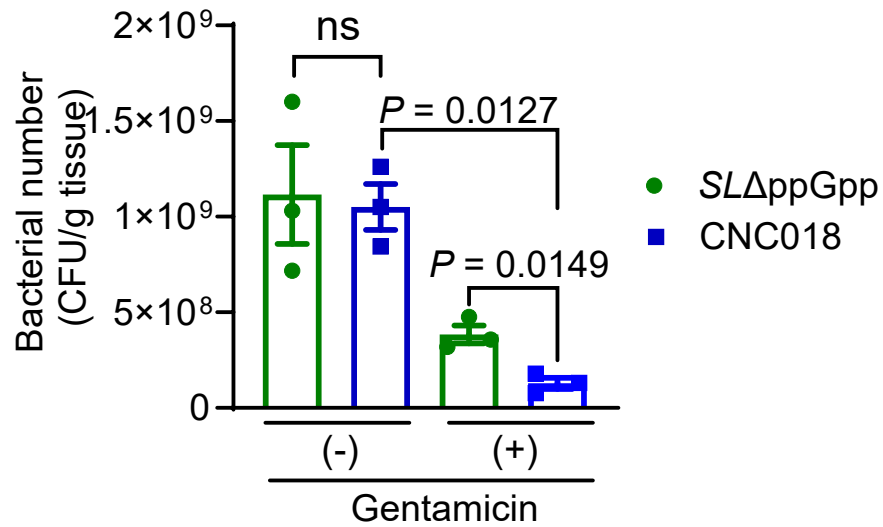


Figure S1. *In vivo* invasion of tumor-colonizing bacteria in CT26 tumors measured by gentamicin-protection assay (related to Figure 1E). BALB/c mice carrying CT26 tumors (volume ~120 mm³) were intravenously administered either *SLΔppGpp* or CNC018 (2×10^7 CFU) on day 0. Tumors were excised, weighed, and homogenized on day 3, and bacterial burden was quantified as CFU/ gram of tumor tissue (CFU/g). For the invasion (intracellular) fraction, matched homogenate aliquots were incubated with gentamicin (300 μ g/mL) for 1 - 2 h at 37 °C (Gentamicin +) to eliminate extracellular bacteria; untreated aliquots (Gentamicin -) represent total recoverable bacteria ($n = 3$ mice/group; ns, not significant; unpaired two-tailed *t*-test).

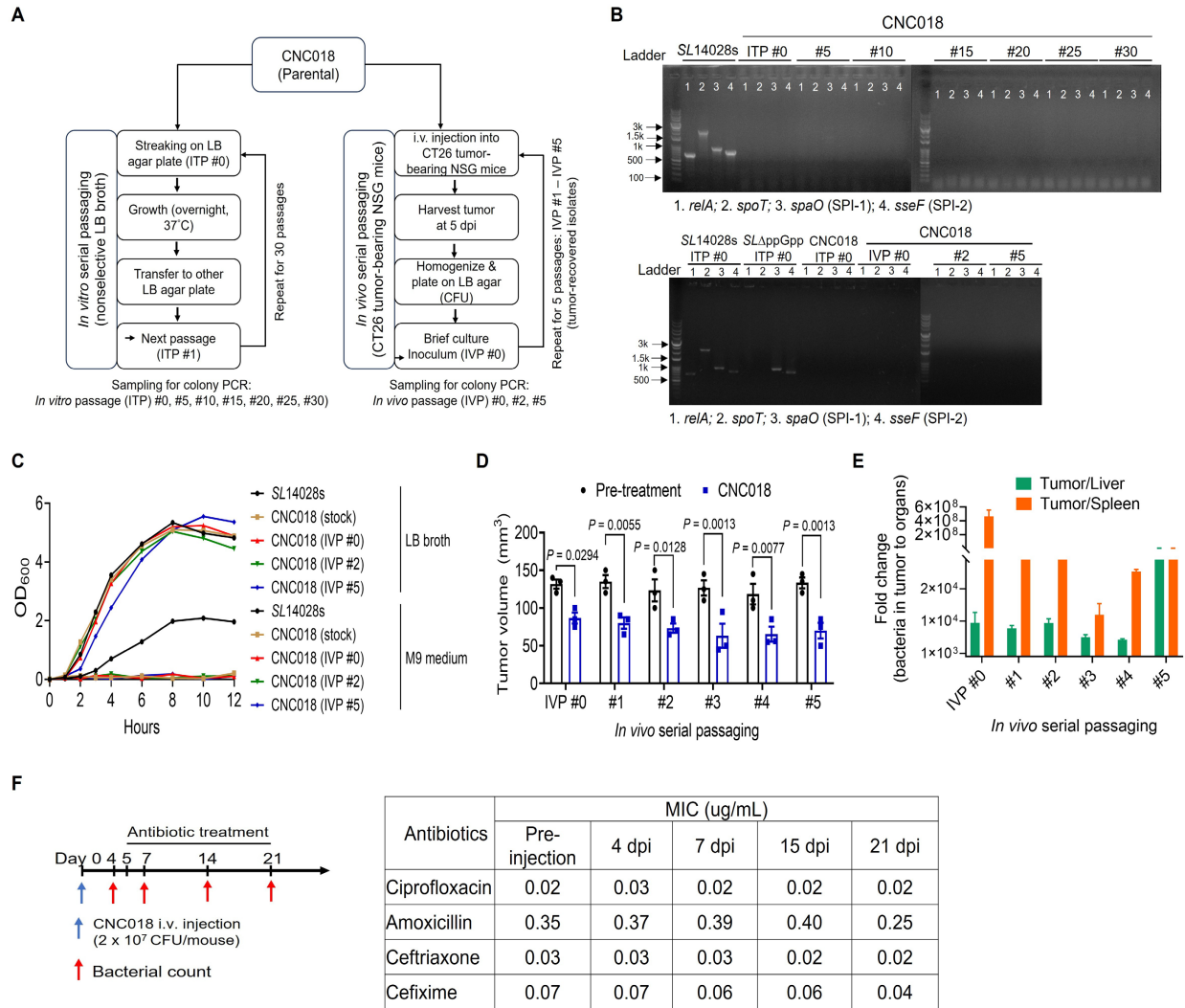


Figure S2. Genetic stability and safety of CNC018 during serial passaging. (A) Schematic of the stability study design (CNC018 serial passaging). To evaluate potential virulence reactivation under maximal selective pressure, CNC018 was subjected to 30 passages in nonselective LB broth (*in vitro*) and five consecutive passages in CT26 tumor-bearing NSG mice (*in vivo*). For *in vivo* passaging, bacteria were isolated from harvested tumors at 5-day post-injection (dpi), cultured briefly, and used as the inoculum for the subsequent round of tumor-bearing NSG mice. (B) PCR genotyping of the engineered deletions. Colony PCR from *in vitro* cultures (*in vitro* passage, ITP #0, #5, #10, #15, #20, #25, #30) (top) and intratumoral isolates recovered from each of the five passages (*in vivo* passage, IVP #0, #2, #5) (bottom). PCR amplicons for regions within *reIA*, *spoT*, *spaO* (SPI-1), and *sseF* (SPI-2) were absent across all samples, confirming the permanent maintenance of the attenuation-associated deletions. WT14028S and *SLΔppGpp* were used as a positive control. (C) Preservation of auxotrophy and metabolic attenuation. Growth curves of the original CNC018 and the tumor-recovered isolate (IVP #0, #2, #5) were compared in nutrient-rich LB broth and M9 minimal medium. Both strains showed identical growth kinetics in LB and remained unable to proliferate in M9, demonstrating that the metabolic requirements for attenuation were not bypassed by compensatory mutations. (D) Antitumor activity from each of the five recovered isolates ($n = 3$ mice/passage; two-way ANOVA with Tukey's multiple comparisons test). (E)

Tumor-preferential colonization. Fold change of bacterial burden in tumors relative to the liver or spleen across the five *in vivo* passages ($n = 3$ mice/passage). (F) Antibiotic susceptibility profile. CT26 tumor-bearing mice received CNC018 (2×10^7 CFU) via i.v. injection when the tumor reached approximately 100-120 mm³ in volume (day 0). Antibiotic treatment (ciprofloxacin, amoxicillin, ceftriaxone, and cefixime) was started on day 5 (60 mg/kg), followed by daily oral dosing of 100 mg/kg. The tumors were collected for bacterial count on days 4, 7, 14, and 21 ($n = 3$ mice/time point) to evaluate antibiotic-dependent clearance of CNC018 in tumor-bearing mice. Left: Experimental scheme; right: Minimum Inhibitory Concentrations (MICs) for clinical antibiotics remain unchanged from pre-treatment through 21 dpi, confirming that CNC018 did not acquire antibiotic resistance during prolonged residence in the tumors.

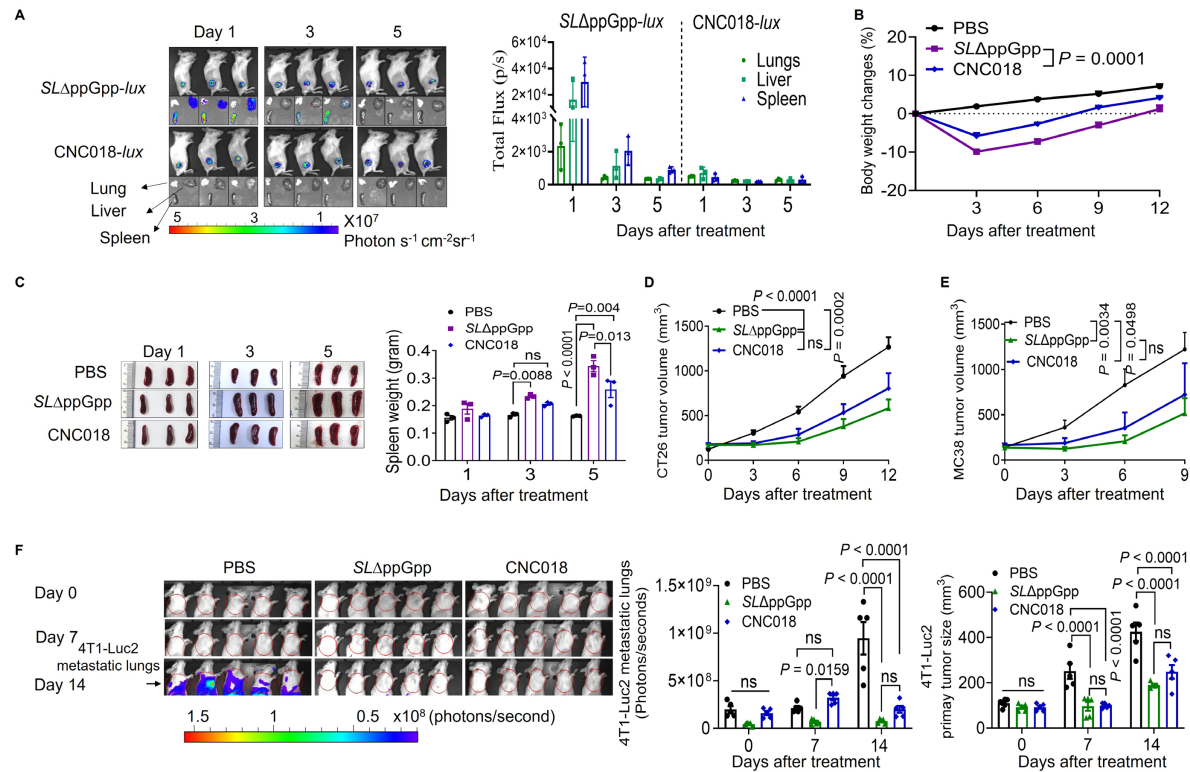


Figure S3. *In vivo* characterizations of CNC018 (related to Figure 1). CT26, MC38, or 4T1-Luc2 tumor cells were implanted s.c. into mice. When tumor volume reached approximately 120 mm³ (day 0), mice received CNC018 via i.v. injection. **(A)** Tumor-colonizing bacteria in mice. *SLΔppGpp-lux* or *CNC018-lux* (4×10^7 CFU/mouse), bioluminescent strains transformed with the *lux* operon, were injected i.v. into BALB/c mice bearing CT26 tumors ($n = 3$ mice/group). Luminescence images of whole mice and normal tissues (lungs, liver, and spleen) were acquired on days 1, 3, and 5 post-bacterial injections. Left, representative images; right, quantification of bioluminescence signals in normal organs. **(B)** Body weight changes of mice treated with PBS, *SLΔppGpp*, or CNC018 (2×10^7 CFU/mouse) ($n = 7$ mice/group, two independent experiments). **(C)** Splenomegaly of CT26 tumor-bearing mice after bacterial treatment. Left, *ex vivo* spleen images; right, spleen weights ($n = 3$ mice/group). **(D, E)** Comparative tumor progression kinetics in **(D)** CT26-bearing BALB/c mice and **(E)** MC38-bearing C57BL/6 mice ($n = 7$ per group, two independent experiments). **(F)** Assessment of 4T1-Luc2 metastatic burden and primary tumor growth. On days 0, 7, and 14 post-treatment, mice received D-luciferin (150 mg/kg, i.p.) for bioluminescence visualization. Representative images (left), quantified luciferase activity of pulmonary metastases (middle), and primary tumor volumes (right) are displayed ($n = 5$ mice/group). Data in B-F were analyzed via two-way ANOVA followed by Tukey's multiple comparisons test; ns, not significant.

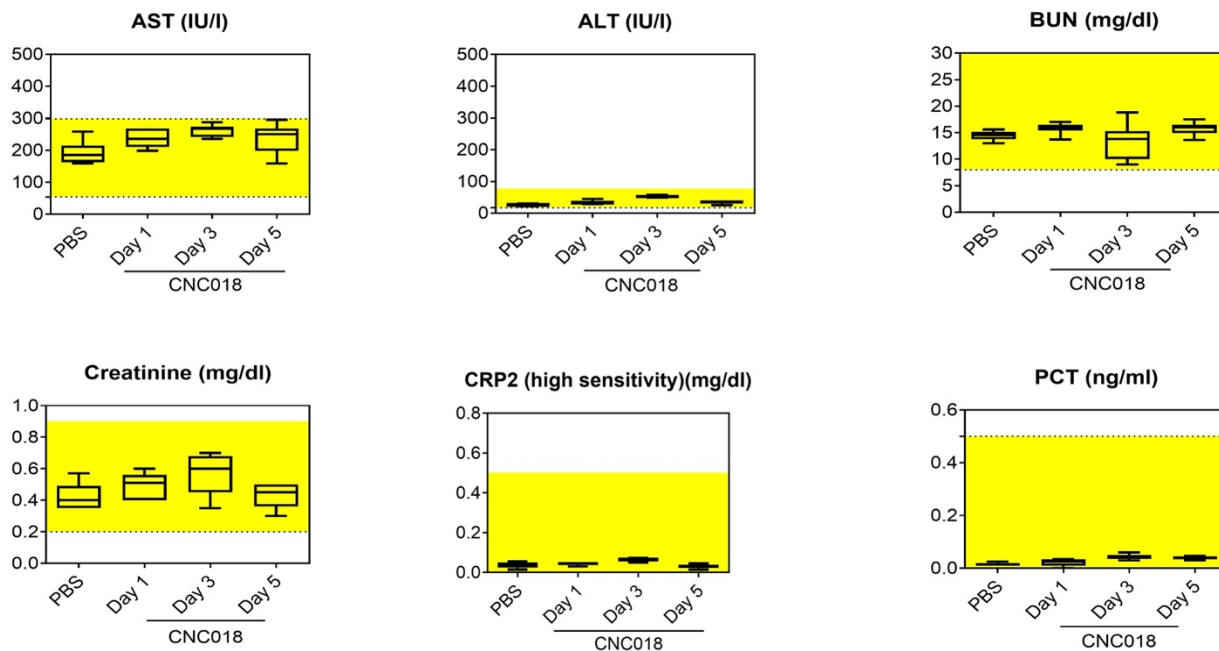


Figure S4. Systemic toxicity of CNC018. BALB/c mice carrying CT26 tumors were intravenously administered CNC018 (2×10^7 CFU per animal; $n = 7$ per group, representative of two independent experimental trials) on day 0. To evaluate organ function and systemic inflammation, serum concentrations of alanine aminotransferase (ALT), aspartate aminotransferase (AST), blood urea nitrogen (BUN), and creatinine, alongside plasma levels of C-reactive protein 2 (CRP2) and procalcitonin (PCT), were quantified at 1, 3, and 5 days post-administration. The yellow-shaded regions represent the standard physiological reference ranges for each respective biomarker.

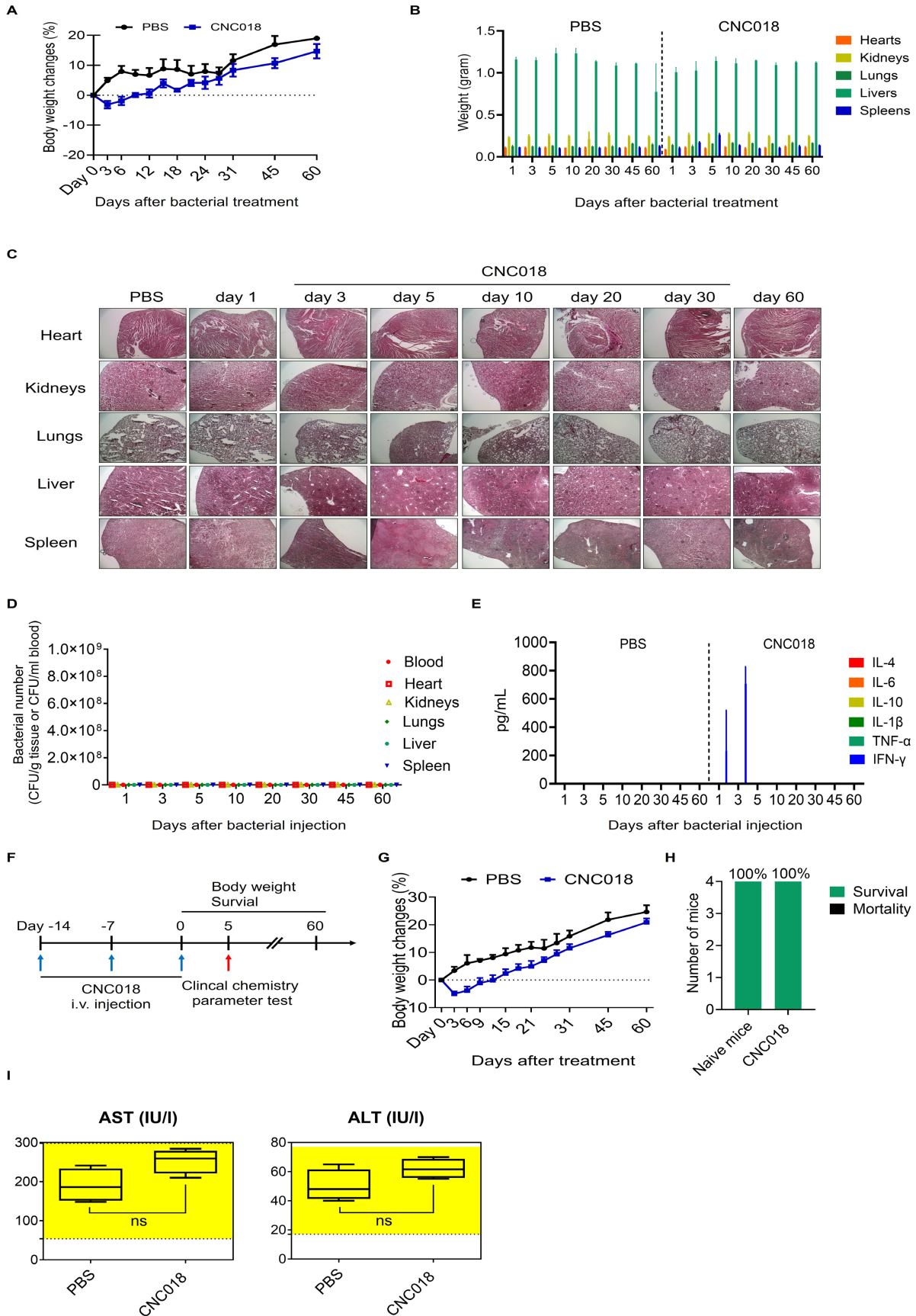


Figure S5. Systemic safety and long-term tolerability of CNC018. Naïve BALB/c mice were treated with PBS or CNC018 (2×10^7 CFU, i.v. injection) and monitored for 60 days. **(A)** Body weight changes of mice expressed as percent of baseline (Day 0) ($n = 4$ mice/group for PBS, $n = 5$ mice/group for CNC018). **(B)** The weight changes of organs post-treatment ($n = 3$ mice/group). **(C)** Representative H&E images of organs (heart, kidneys, lungs, liver, spleen) were collected on days 1, 3, 5, 10, 20, 30, and 60. **(D)** Bacterial burdens in organs at indicated time points quantified as CFU/g tissue. **(E)** Serum cytokines measured at indicated times post-treatment ($n = 3$ mice/group). **(F - I)** The sustained biosafety of CNC018 in a therapeutic repeat-dosing study for long-term observation. **(F)** Schematic of the triple-dose toxicity study. BALB/c mice ($n = 4$ mice/group) received i.v. injections of CNC018 (2×10^7 CFU) or PBS for triple-dose. **(G)** Body weight change during treatment. **(H)** Survival of mice after 60 post-treatments from (F). **(I)** Quantification of serum AST and ALT levels on day 5. Yellow shading indicates normal reference ranges for each parameter. Statistical significance was determined using an unpaired two-tailed *t*-test; ns, not significant.

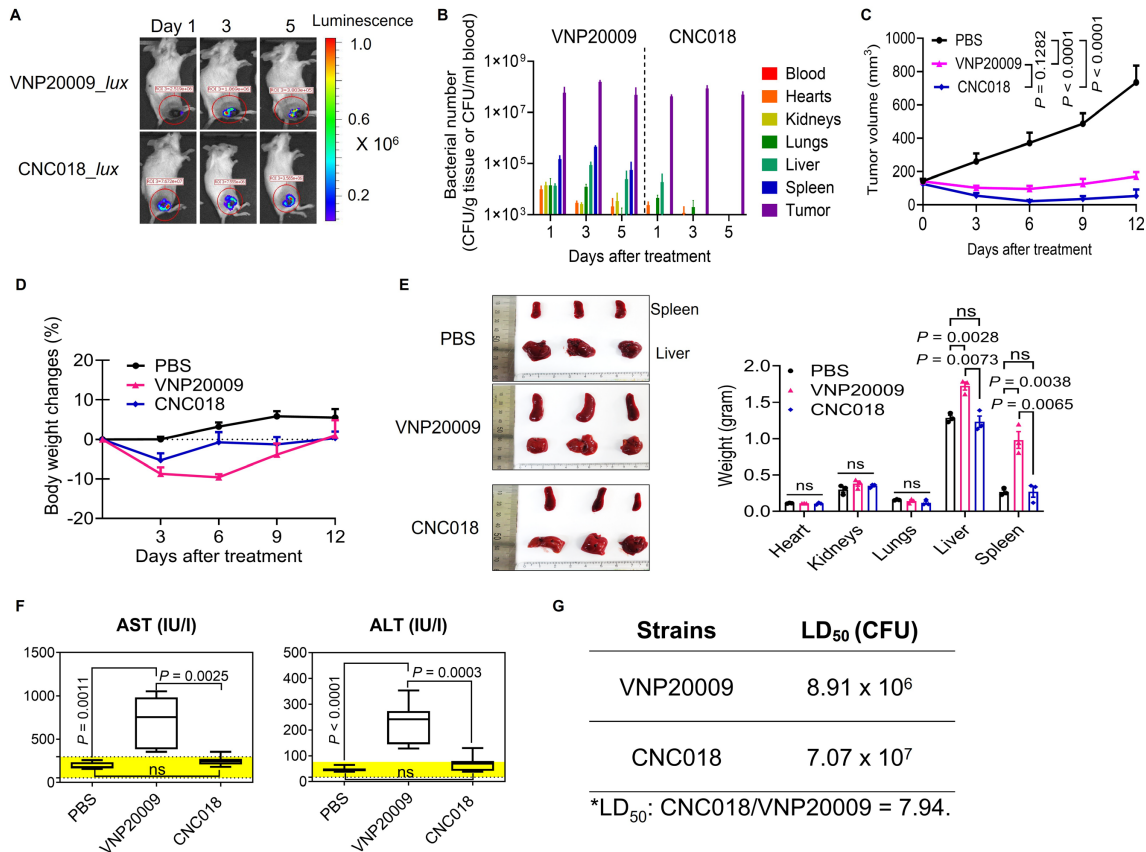


Figure S6. Biosafety and antitumor effects of VNP20009 and CNC018. (A&B) Tumor-colonizing bacteria in mice. CNC018-*lux*, VNP20009-*lux*, VNP20009, or CNC018 (2×10^7 CFU/mouse) were injected i.v. into BALB/c mice bearing CT26 tumors ($n = 3$ mice/group) (day 0). (A) Luminescence images of mice treated with CNC018-*lux* and VNP20009-*lux* were acquired at 1, 3, and 5 dpi ($n = 3$ mice/group). (B) Bacterial count of CNC018 and VNP20009 at 1, 3, and 5 dpi ($n = 3$ mice/group). (C) Average growth curves of tumors in mice treated with PBS, VNP2009, or CNC018. (D) Body weight changes of mice after bacterial treatment. P -values in C-D were determined by two-way ANOVA with Tukey's multiple comparisons test ($n = 4$ mice/group; ns, not significant). (E) Organ weight after bacterial treatment on day 3. Left: *ex vivo* spleen and liver images; right: spleen and liver weights ($n = 3$ /group). (F) Serum levels of aspartate aminotransferase (AST) and alanine aminotransferase (ALT) were measured on day 3 after treatment. Yellow shading indicates normal reference ranges for each parameter ($n = 7$ mice/group). P -values in E-F were determined by an unpaired two-tailed t -test; ns, not significant. (G) Median lethal dose (LD₅₀) in mice following bacterial infection. BALB/c mice ($n = 5$ mice/group) were treated with VNP20009 or CNC018 via i.v. injection. Mouse survival was monitored for 30 days to determine the LD₅₀ using the Reed and Muench method.

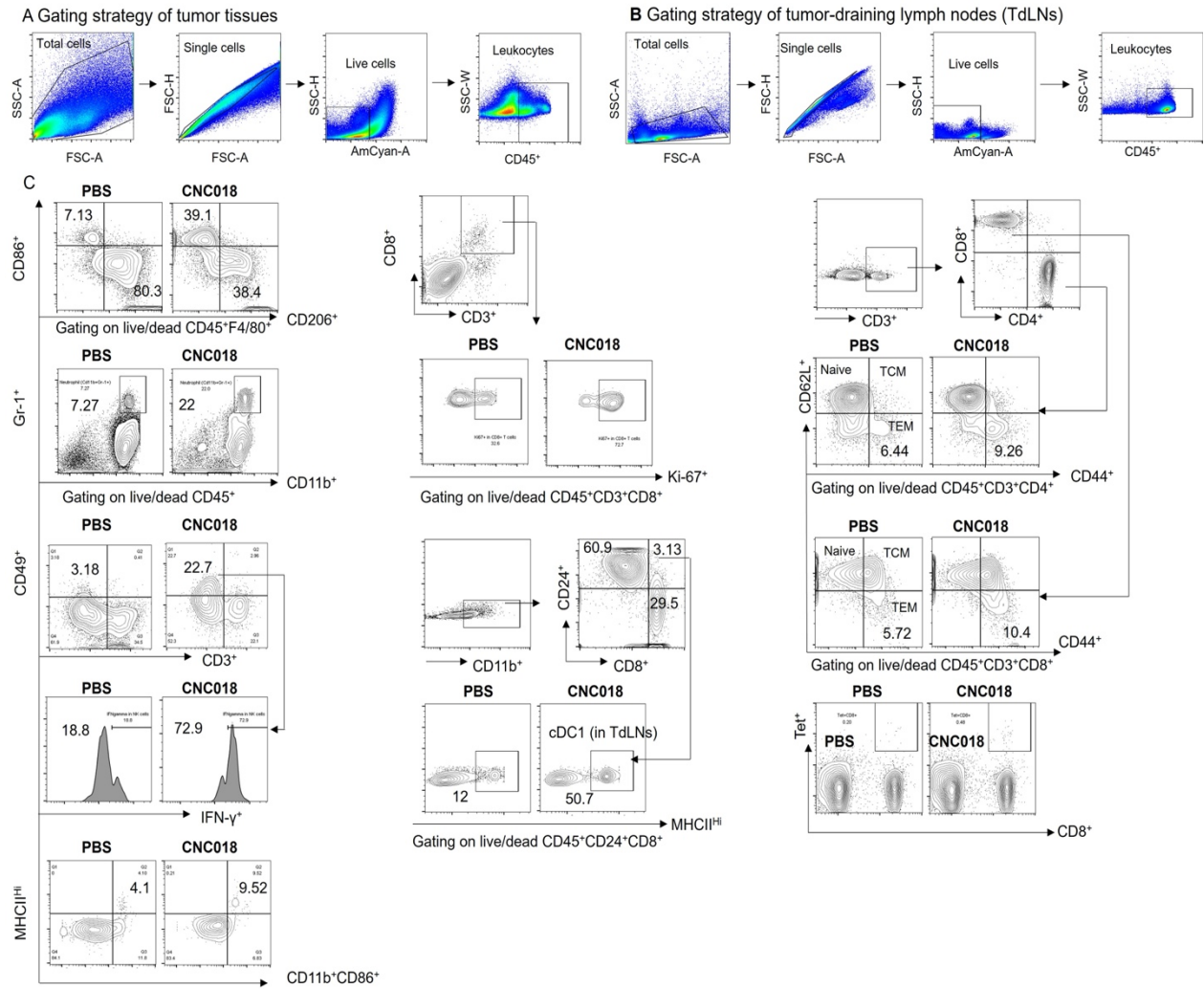


Figure S7. Gating strategies of flow cytometry analysis (related to Figure 2). Immune cells were harvested from CT26 tumors and TdLNs. Cells were identified by flow cytometry after staining with a Live/Dead cell kit, anti-CD45 (leukocyte marker), anti-CD16/CD32 (to block non-specific Fc receptor binding), and additional immune cell-specific markers. **(A)** Gating strategy for tumor tissue analysis. **(B)** Gating strategy for TdLN analysis. **(C)** Immune cell profiles determined from gates shown in (A) and (B).

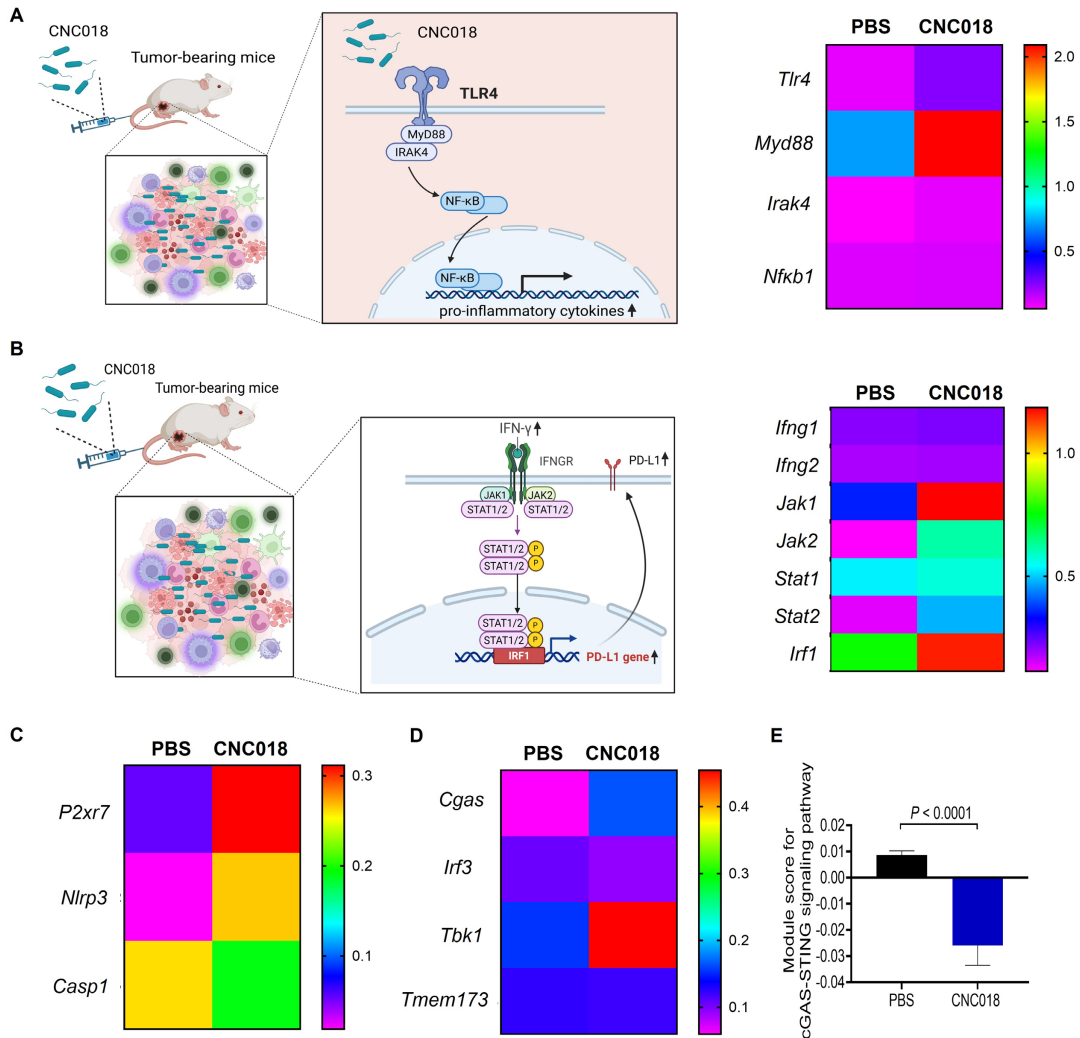


Figure S8. CNC018-induced pro-inflammatory responses are mediated by the stimulation of multiple signaling pathways in the TME (related to Figure 2P-R). BALB/c mice carrying CT26 tumors were intravenously challenged with either PBS or CNC018 (2×10^7 CFU) once tumors reached a volume of ~ 120 - 140 mm^3 (designated as day 0). Tumors were harvested on day 3 for scRNA-seq analysis ($n = 2$ pooled tumors per group). **(A)** Schematic diagram of a signaling pathway relating CNC018-induced pro-inflammatory cytokines (left); heatmaps show representative mRNA gene expression of TLR4 signaling, including 4 genes (*Tlr4*, *Myd88*, *Irak4*, and *Nfkb1*) (right). **(B)** Schematic diagram of the signaling pathway relating to the CNC018-induced IFN- γ signaling pathway (left); heatmaps show representative mRNA gene expression of IFN- γ signaling, including 7 genes (*lfng1*, *lfng2*, *Jak1*, *Jak2*, *Stat1*, *Stat2*, and *Irf1*) (right). **(C)** Heatmaps show representative mRNA gene expression of inflammasome activation (*P2xr7*,

Nlrp3, and *Casp1*), and (D) heatmaps show representative mRNA gene expression of the cGAS–STING signaling pathway (*Cgas*, *Irf3*, *Tbk1*, and *Tmem173*). (E) The mRNA levels of signaling module scores from (D) (n = 2 combined tumors for each group; unpaired two-tailed *t*-test).

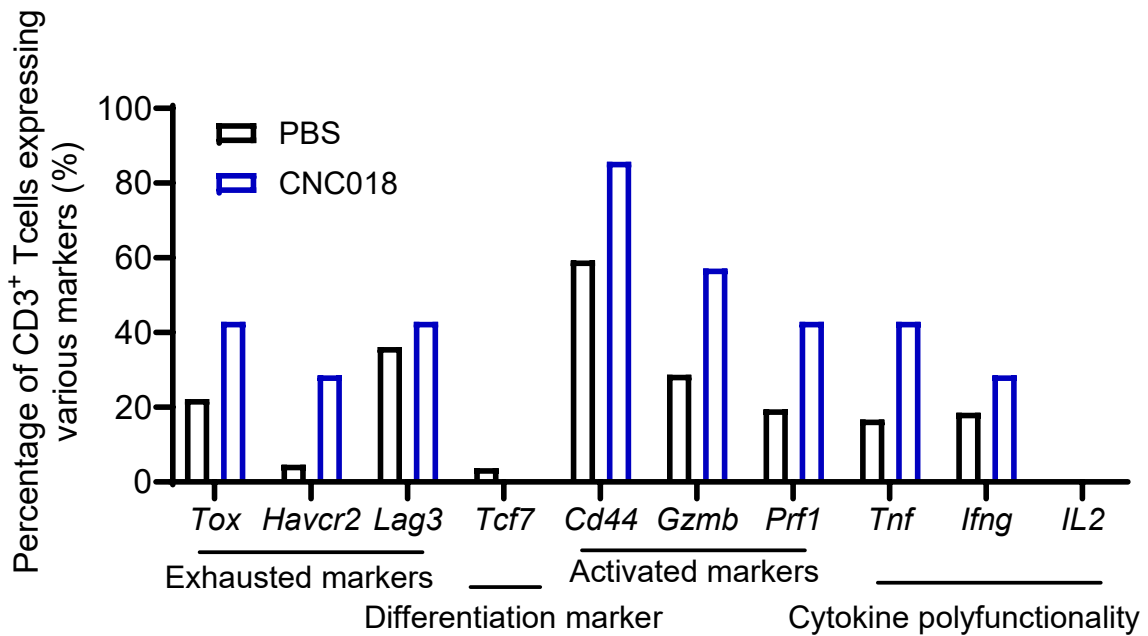


Figure S9. ScRNA-seq analysis of marker and cytokine transcript expression in CD3⁺ T cells infiltrating tumors. scRNA-seq was performed on CT26 tumors in mice treated with PBS or CNC018 ($n = 2$ pooled tumors per group) on day 3 after bacterial treatment. Bar plots show the frequencies of CD3⁺ T cells expressing *Tox* (TOX), *Havcr2* (TIM3), *Lag3* (LAG3), *Tcf7* (TCF-1), *Cd44* (CD44), *Gzmb* (GzmB), *Prf1* (Perforin), *Tnf* (TNF- α), *Ifng* (IFN- γ), and *Il2* (IL-2) mRNA in the PBS and CNC018 groups. The markers are grouped according to exhaustion, differentiation, activation, and cytokine polyfunctionality, as indicated in the figure.

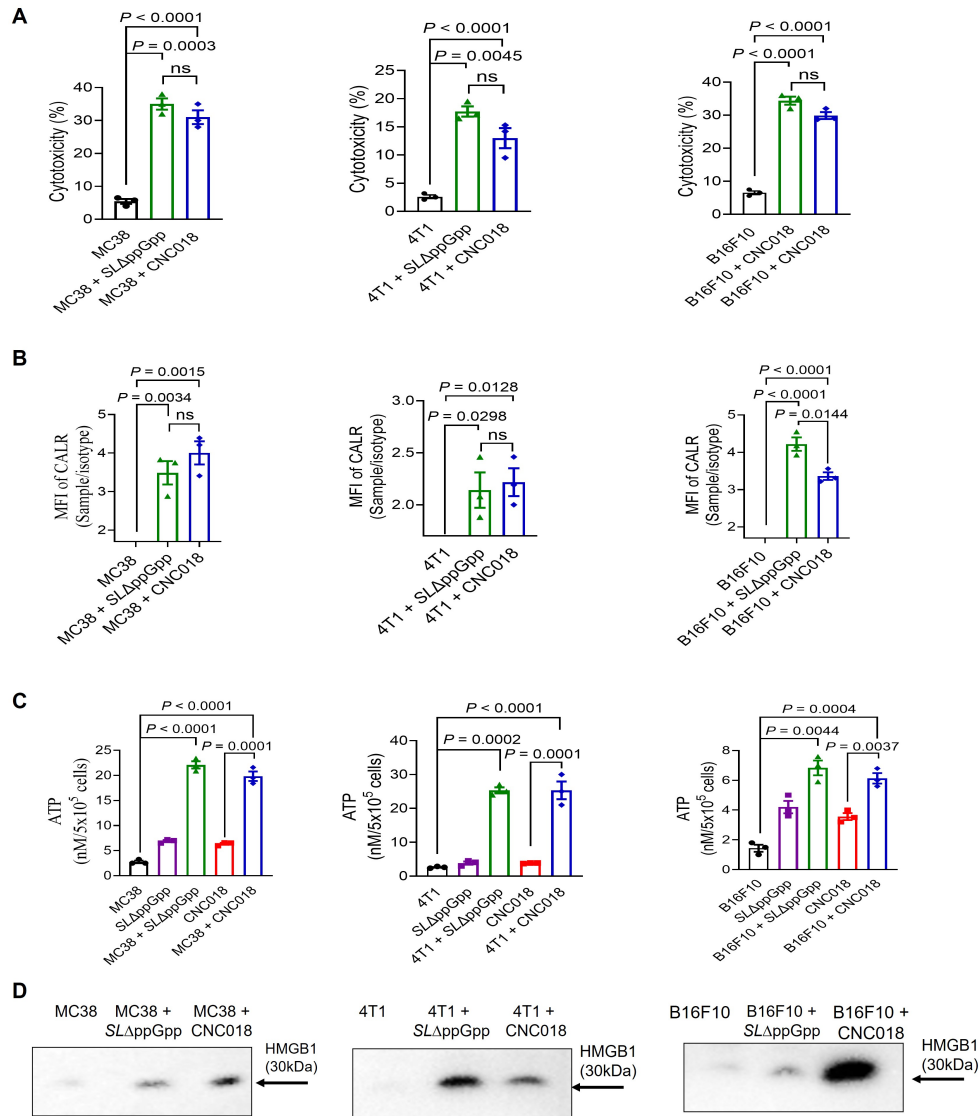


Figure S10. DAMPs released from CNC018-induced dying tumor cells (related to Figure 3A-D). CT26, MC38, 4T1, or B16F10 cells (1×10^5) were cultured in antibiotic-free complete medium for 14-16 h, then treated with PBS, SL Δ ppGpp, or CNC018 (1×10^6 CFU) in antibiotic-free medium for an additional 20-24 h. **(A)** Cytotoxicity assay. Cell viability was performed by evaluating lactate dehydrogenase (LDH) release from the supernatant ($n = 3$ technical replicates). **(B)** CALR exposure on the cell surface. Cells were stained with anti-CALR (α CALR) or IgG control, and mean fluorescence intensity (MFI) was measured by flow cytometry ($n = 3$ technical replicates). **(C)** ATP secretion from cancer cells. ATP levels were quantified in the culture supernatant ($n = 3$ technical replicates). P -values in A-C were calculated by an unpaired two-tailed t -test; ns, not significant. **(D)** HMGB1 release from cancer cells. Culture supernatants were analyzed by Western blotting using anti-HMGB1 antibody.

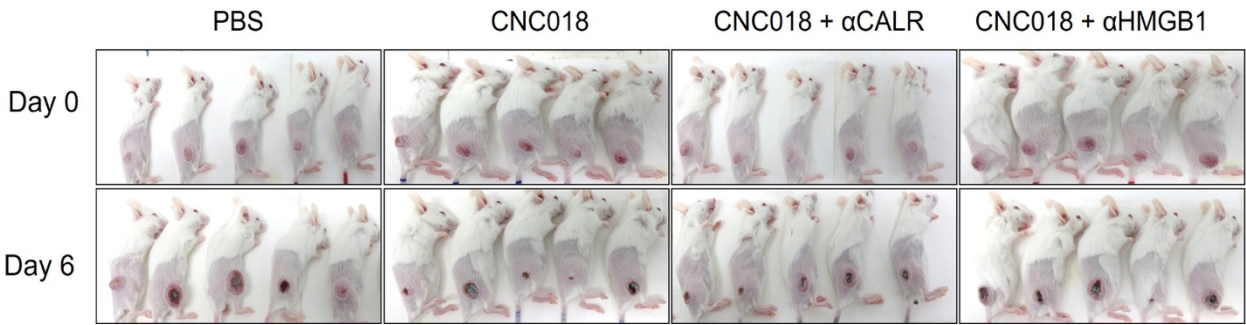


Figure S11. Photos of mice with CT26 tumors taken before and after treatment with CNC018 and anti-DAMP antibodies (related to Figure 3F-J). BALB/c mice underwent subcutaneous inoculation with CT26 cells (5×10^5). Upon reaching a mean tumor volume of $\sim 120 \text{ mm}^3$, subjects were administered either PBS or CNC018 (2×10^7 CFU) through a single tail-vein injection (day 0). To sequester DAMPs, anti-CALR (α CALR) or anti-HMGB1 (α HMGB1) monoclonal antibodies were delivered intraperitoneally on a biweekly schedule (commencing on day -1) for three consecutive doses. Mouse images on days 0 and 6 are shown for each treatment group: PBS, CNC018, CNC018 + α CALR, and CNC018 + α HMGB1.

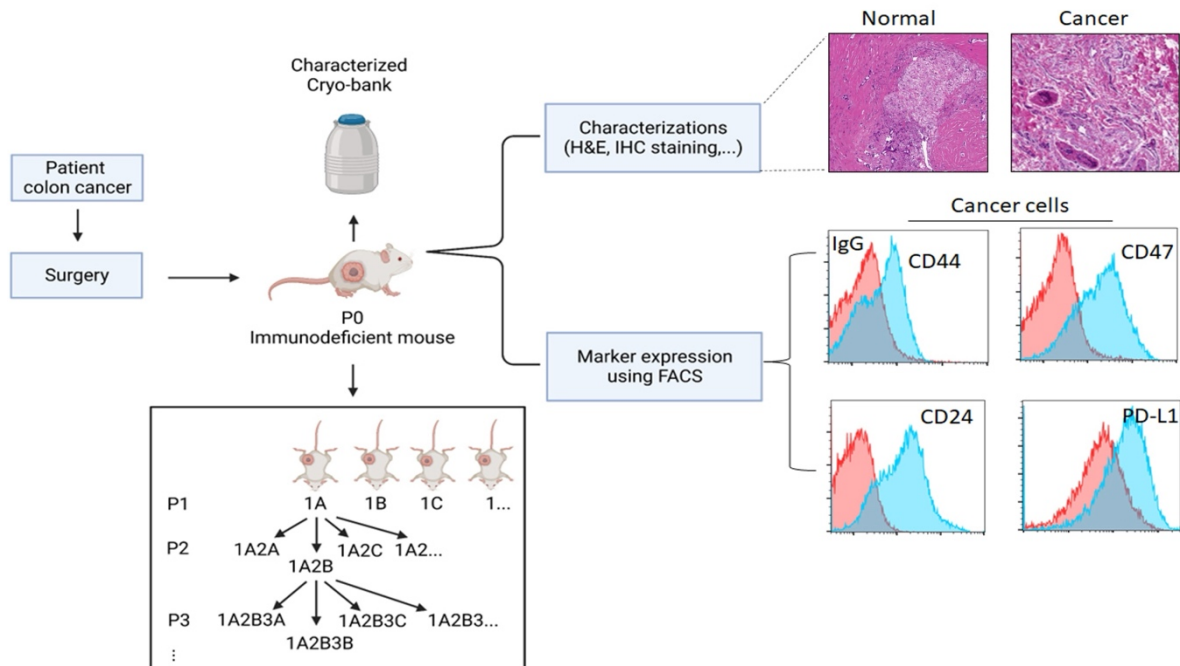


Figure S12. Generation of colon cancer PDX tumor model (related to Figure 4A-H). Surgical specimens from colon cancer patients were divided into small pieces and transplanted s.c. into NSG mice (P0). Tumor xenografts from P0 mice were characterized by hematoxylin and eosin (H&E) staining and flow cytometry, stored in cryobanks for subsequent implantation. Xenografting was repeated in NSG mice (P1 and subsequent passages). Final xenograft mice (P3) were used for subsequent bacterial treatment. Representative micrographs show the H&E staining of normal and tumor tissue (top right). Flow cytometry histograms (bottom right) indicate expression of CD44, CD47, CD24, and PD-L1 on tumor cells (blue) versus IgG control (red). See Materials and Methods for details.

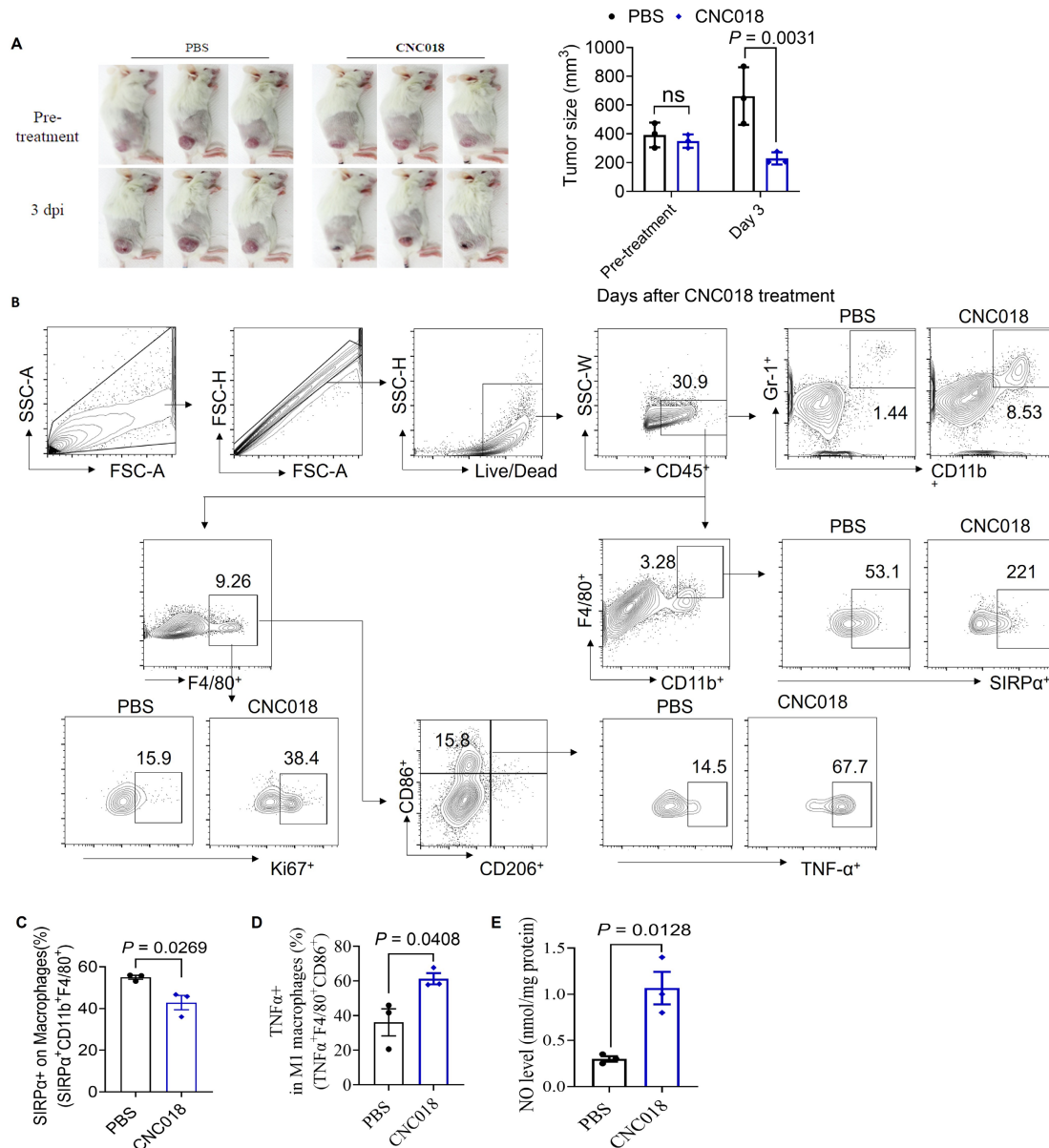


Figure S13. Tumor size and flow cytometry analysis of PDX tumors treated with CNC018 (related to Figure 4A-H). Tumor cells from colorectal cancer patients (1×10^6) were inoculated s.c. into the flank of NSG mice to establish a patient-derived xenograft (PDX) tumor model (P0). After four passages, P3 tumor-bearing mice were injected i.v. with PBS or CNC018 (2×10^7 CFU) when tumor size reached approximately 300 mm³ (day 0). Intratumoral immune cells were analyzed by flow cytometry. **(A)** Tumor size at 0 dpi (pre-treatment) and 3 dpi. Left, representative images of mice; right, tumor volumes ($n = 3$ mice/group; ns, not significant; two-way ANOVA with Tukey's multiple comparisons test). **(B)** Flow cytometry gating strategy. **(C)** Proportion of activated macrophages (SIRPα⁺CD11b⁺F4/80⁺). **(D)**

Frequency of activated M1 macrophages (TNF α ⁺F4/80⁺CD86⁺). (E) NO concentrations in tumor lysates. *P*-values in C-E were detected by an unpaired two-tailed *t*-test (*n* = 3 mice/group).

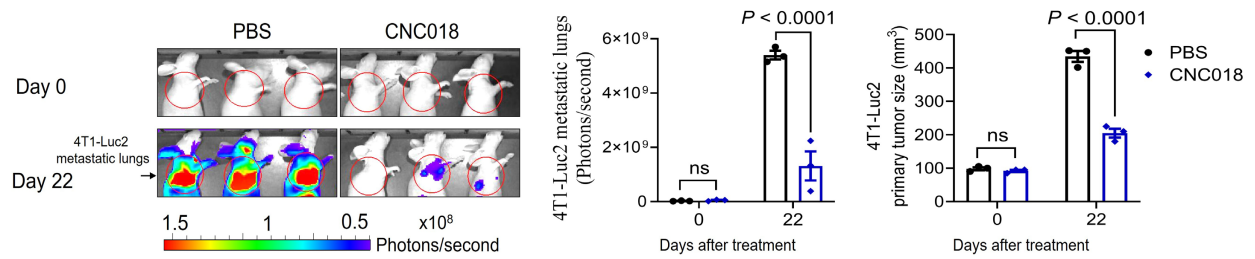


Figure S14. CNC018 suppresses growth of primary and metastatic murine tumors. BALB/c athymic *nu/nu* mice were implanted s.c. with 4T1-Luc2 cells (5×10^5). When primary tumor volumes reached 120 - 140 mm³, mice received PBS or CNC018 (2×10^7 CFU/mouse) via i.v. injection (day 0). *In vivo* bioluminescence imaging was performed after i.p. injection of D-luciferin (150 mg/kg, FLuc activity). Left: Longitudinal macroscopic bioluminescence imaging of representative mice at baseline (day 0) and day 22. Middle: Assessment of metastatic load in the lungs based on bioluminescence signal intensity on days 0 and 22. Right: Statistical comparison of primary tumor volumes on days 0 and 22 ($n = 3$ mice/group; ns, not significant; analysis via two-way ANOVA with Tukey's multiple comparisons test).

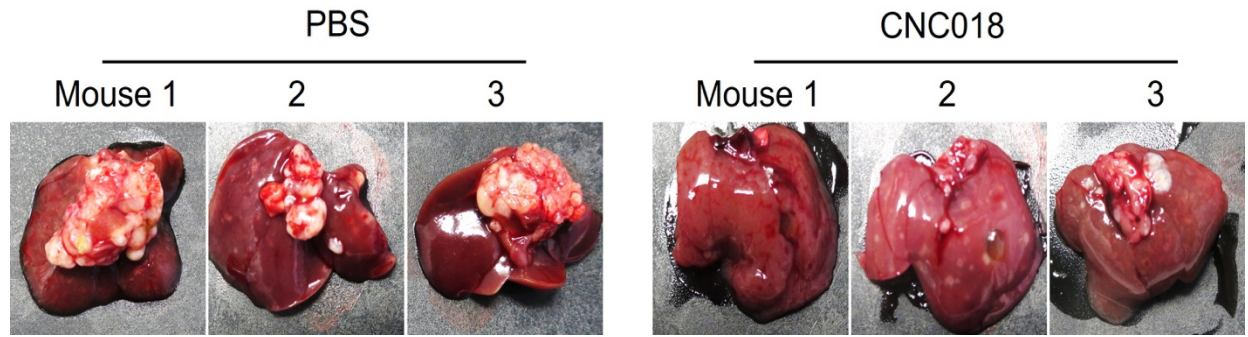


Figure S15. CNC018 inhibits liver metastasis (related to Figure 4I). Liver metastases were established by i.p. injection of human hepatoma HepG2-Fluc cells (3×10^5) into immunocompromised athymic *nu/nu*⁻ BALB/c mice. Three days after tumor implantation, CNC018 (2×10^7 CFU) was administered via i.v. injection (day 0). Representative *ex vivo* images of livers were harvested at the experimental endpoint (day 29) (n = 3 mice/group).

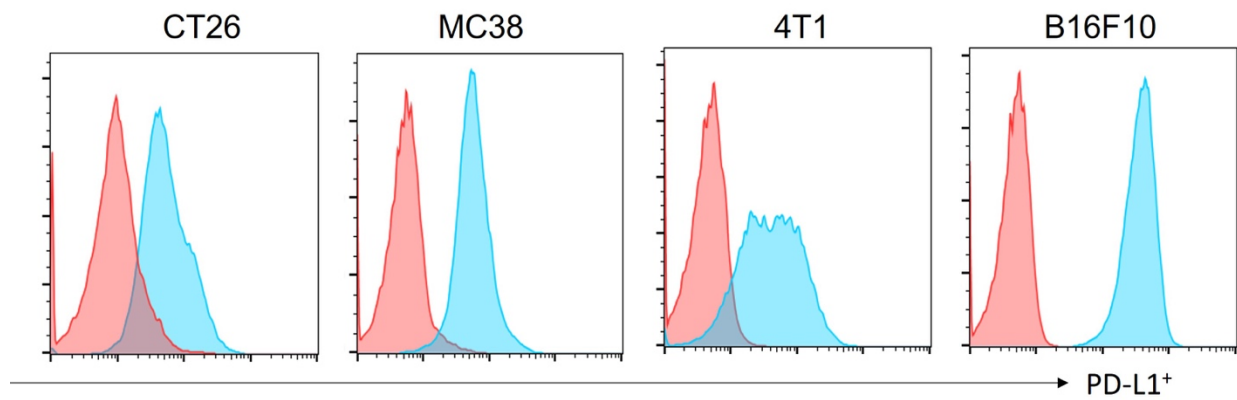


Figure S16. PD-L1 expression on cancer cell lines (CT26, MC38, 4T1, B16F10) *in vitro* (related to Fig. 5A). Cells were stained with IgG control antibody (red) or anti-PD-L1 antibody (green) and analyzed by flow cytometry.

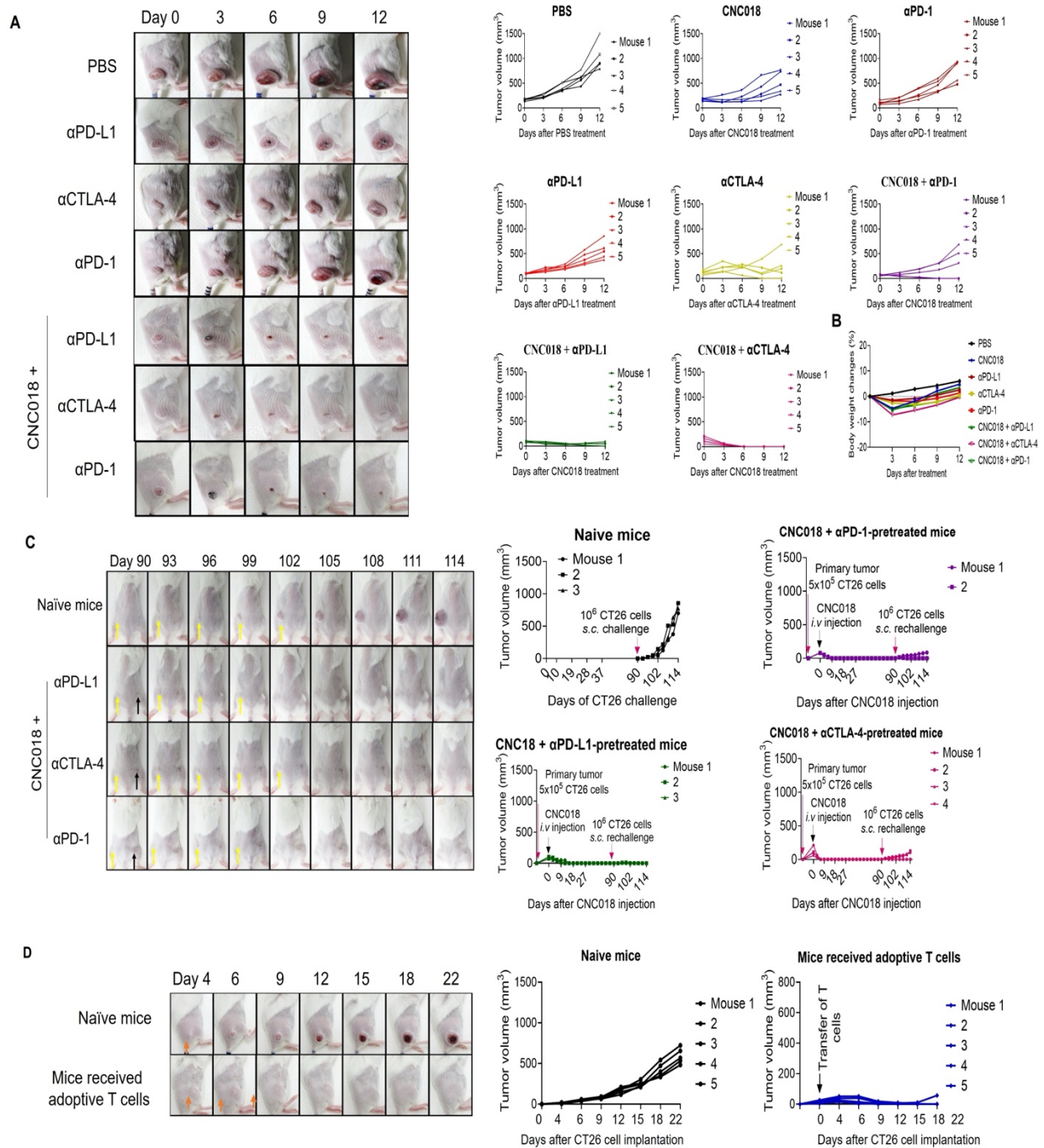


Figure S17. CNC018 strongly potentiates the anti-tumor efficacy of ICB against CT26 tumors (related to Figure 5I-L). CT26 cells were inoculated s.c. into the flank of BALB/c mice. Tumor-bearing mice received CNC018 (2×10^7 CFU) via i.v. injection (day 0) and/or ICBs via i.p. injection (200 μ g/mouse, twice weekly for five doses, starting on day -1). The anti-CD8 (α CD8) antibody was injected i.p. to deplete CD8⁺ T cells. Tumor-eradicated mice were rechallenged by s.c. implantation of CT26 cells

(1×10^6) into the contralateral flank on day 90; black arrows indicate the implantation sites. Naïve age-matched mice were used as controls ($n = 3$ mice). Separately, CT26 cells were implanted s.c. into the right hind flanks of mice (day 0). Adoptive transfer of T-cells (1×10^6) from tumor-eradicated mice was transferred into tumor-bearing mice on day 4. **(A)** Representative images (left) and individual tumor growth curves (right) of each treated group (related to Figure 5I-K). **(B)** The changes of body weight after treatment. **(C)** Representative images (left) and individual growth curves of primary and rechallenged tumors (right) in naïve and tumor-eradicated mice (related to Fig. 5L). Scars of primary tumors and rechallenge sites are marked by black and yellow arrows, respectively. **(D)** Representative images (left) and individual tumor growth curves (middle and right) of mice receiving adoptive T-cells from tumor-eradicated mice (related to Fig. 5N).

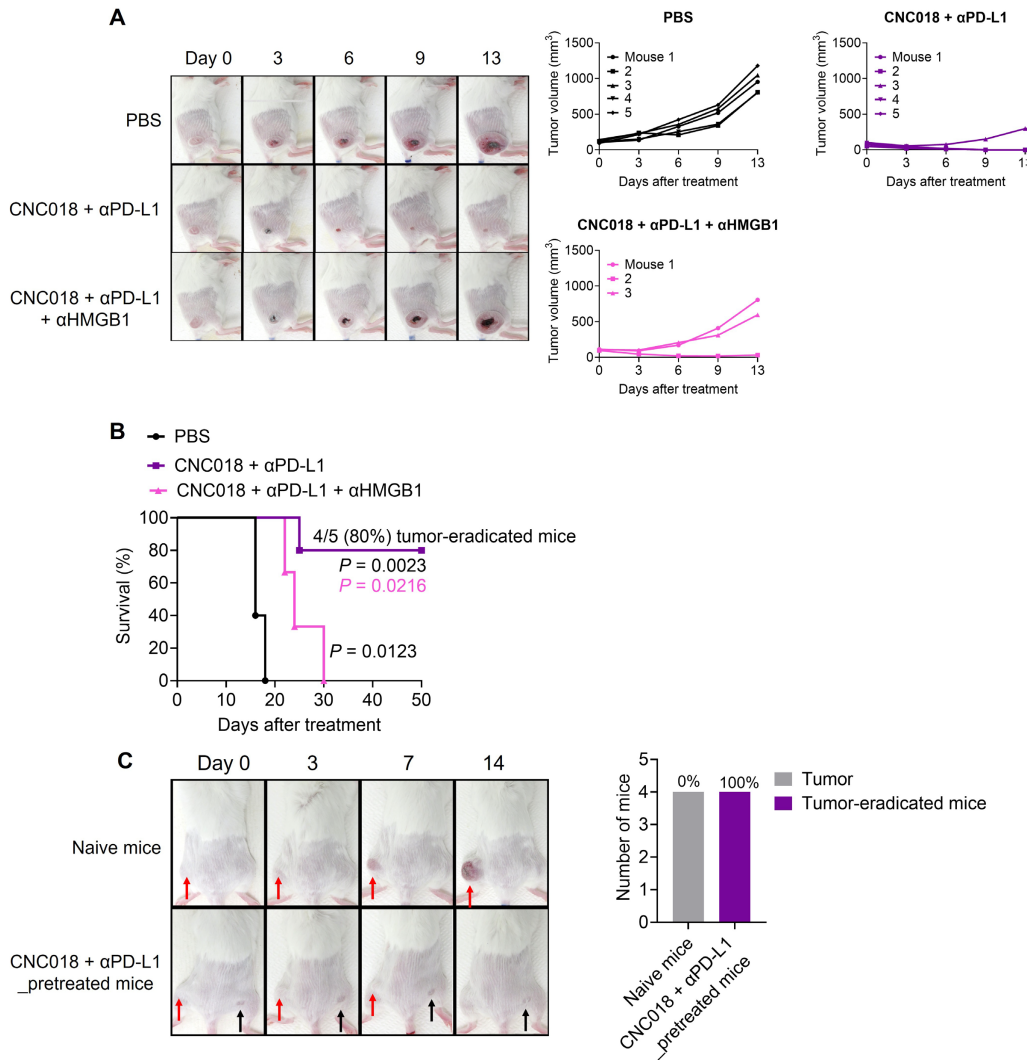


Figure S18. HMGB1 is required for the combination of CNC018 and αPD-L1 antibody to suppress tumors (related to Figure 5O). CT26 cells were inoculated s.c. into the right hind flank of BALB/c mice. Tumor-bearing mice received CNC018 (2×10^7 CFU) via *i.v.* injection (day 0) and/or ICBs via *i.p.* injection (200 μg/mouse, twice weekly for five doses, starting on day -1). For HMGB1 neutralization, an αHMGB1 antibody (20 μg/mouse) was injected *i.p.* (twice weekly for three doses, starting on day -1). **(A)** Left: representative images; Right: individual tumor growth curves of each treatment group. **(B)** Kaplan-Meier survival curves of CT26 tumor-bearing BALB/c mice from (A) [$n = 3 - 5$ mice/group; log-rank (Mantel-Cox) test]. **(C)** Representative images (left) and percentages of mice without recurrence of secondary tumors after tumor rechallenge (right) in naïve and tumor-eradicated mice after treatment with CNC018 + αPD-L1 for 50 days. Scars of primary tumors and rechallenge sites are marked by black and red arrows, respectively ($n = 4$ mice/group).

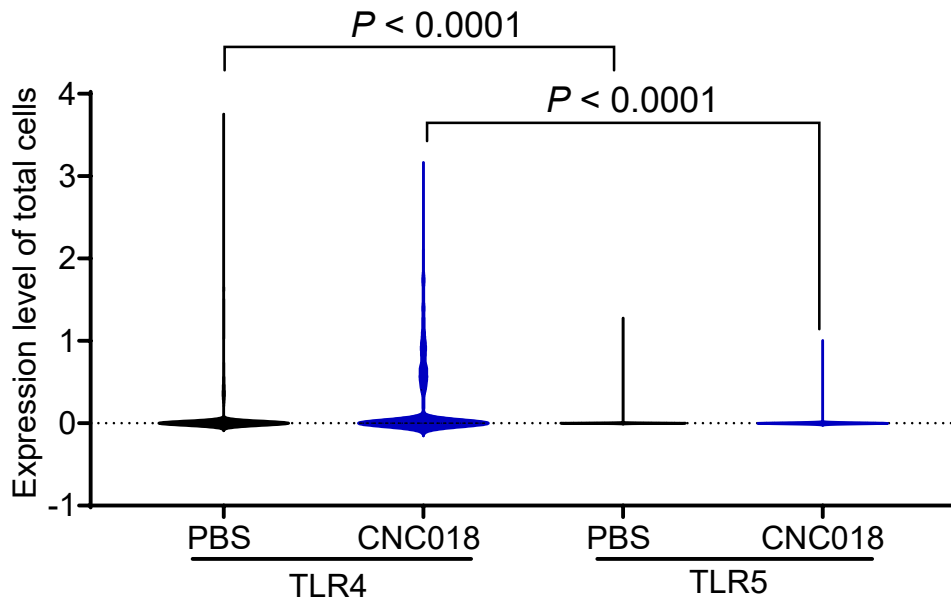


Figure S19. ScRNA-seq analysis of TLR4 and TLR5 mRNA expression in total cells from CT26 tumors. Mice bearing CT26 tumor were i.v. injected with PBS or CNC018 (2×10^7 CFU) when tumor size was approximately 120 mm^3 (day 0). Tumors were harvested on day 3 for single-cell RNA sequencing analysis. Violin plots show the expression levels of TLR4 and TLR5 mRNA in total cells from the PBS and CNC018 groups ($n = 2$ pooled tumors/group; unpaired two-tailed t -test).

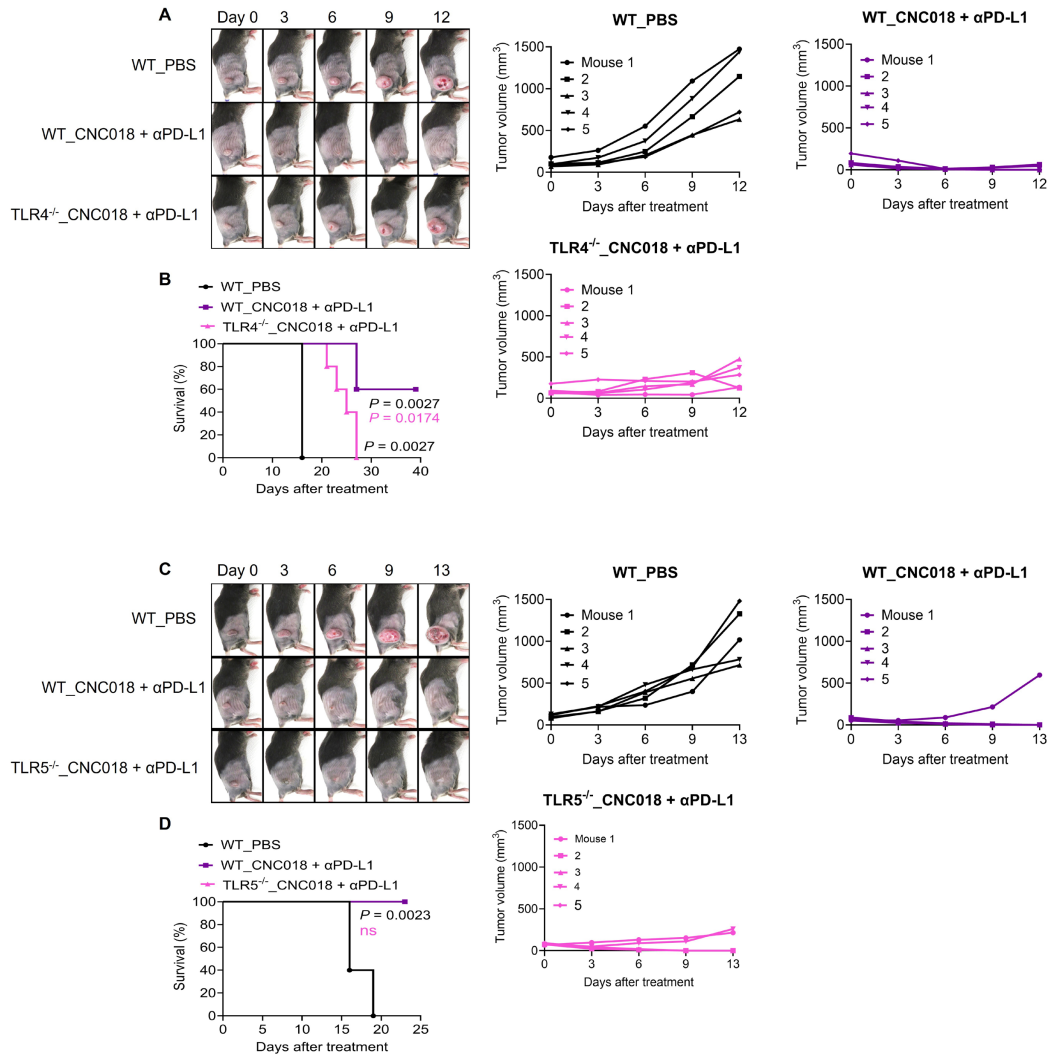


Figure S20. Mechanistic evaluation of CNC018 and αPD-L1 combination therapy in TLR-deficient mouse models (related to Figure 5P-Q). WT, TLR4^{-/-}, and TLR5^{-/-} C57BL/6 mice ($n = 5$ mice/group) were subcutaneously challenged with MC38 tumor cells. Upon reaching a mean tumor burden of ~80-100 mm³, subjects were administered either a combination of CNC018 (2×10^7 CFU, i.v.) and an αPD-L1 antibody or a PBS control on day 0. **(A)** Left: representative images; Right: individual tumor growth curves (right) of each treatment group (WT_PBS, WT_CNC018 + αPD-L1, and TLR4^{-/-}_CNC018 + αPD-L1). **(B)** Kaplan-Meier survival curves of MC38 tumor-bearing C57BL/6 mice from (A) [$n = 5$ mice/group; log-rank (Mantel-Cox) test]. **(C)** Left: representative images; Right: individual tumor growth curves (right) of each treatment group (WT_PBS, WT_CNC018 + αPD-L1, TLR5^{-/-}_CNC018 + αPD-L1). **(D)** Kaplan-Meier survival curves of MC38 tumor-bearing C57BL/6 mice from (C) [$n = 5$ mice/group; ns, not significant; log-rank (Mantel-Cox) test].

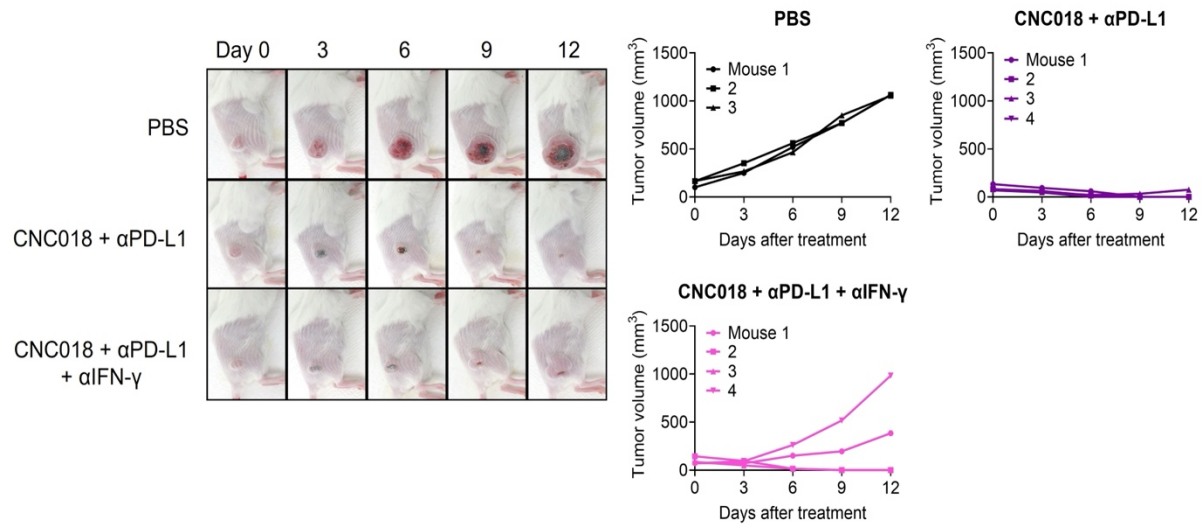


Figure S21. IFN- γ is required for the combination of CNC018 and α PD-L1 antibody to suppress tumors (related to Figure 5R). BALB/c mice were subcutaneously inoculated with 5×10^5 CT26 cells in the right hind flank. Once tumors were established, mice were administered CNC018 (2×10^7 CFU) intravenously (day 0) and/or anti-PD-L1 antibody via intraperitoneal delivery (twice weekly for five doses, starting on day -1). For IFN- γ neutralization, an α IFN antibody (200 μ g/mouse) was injected i.p. (twice weekly for five doses, starting on day -1). Left: representative images (left); Right: individual tumor growth curves of each treatment group.

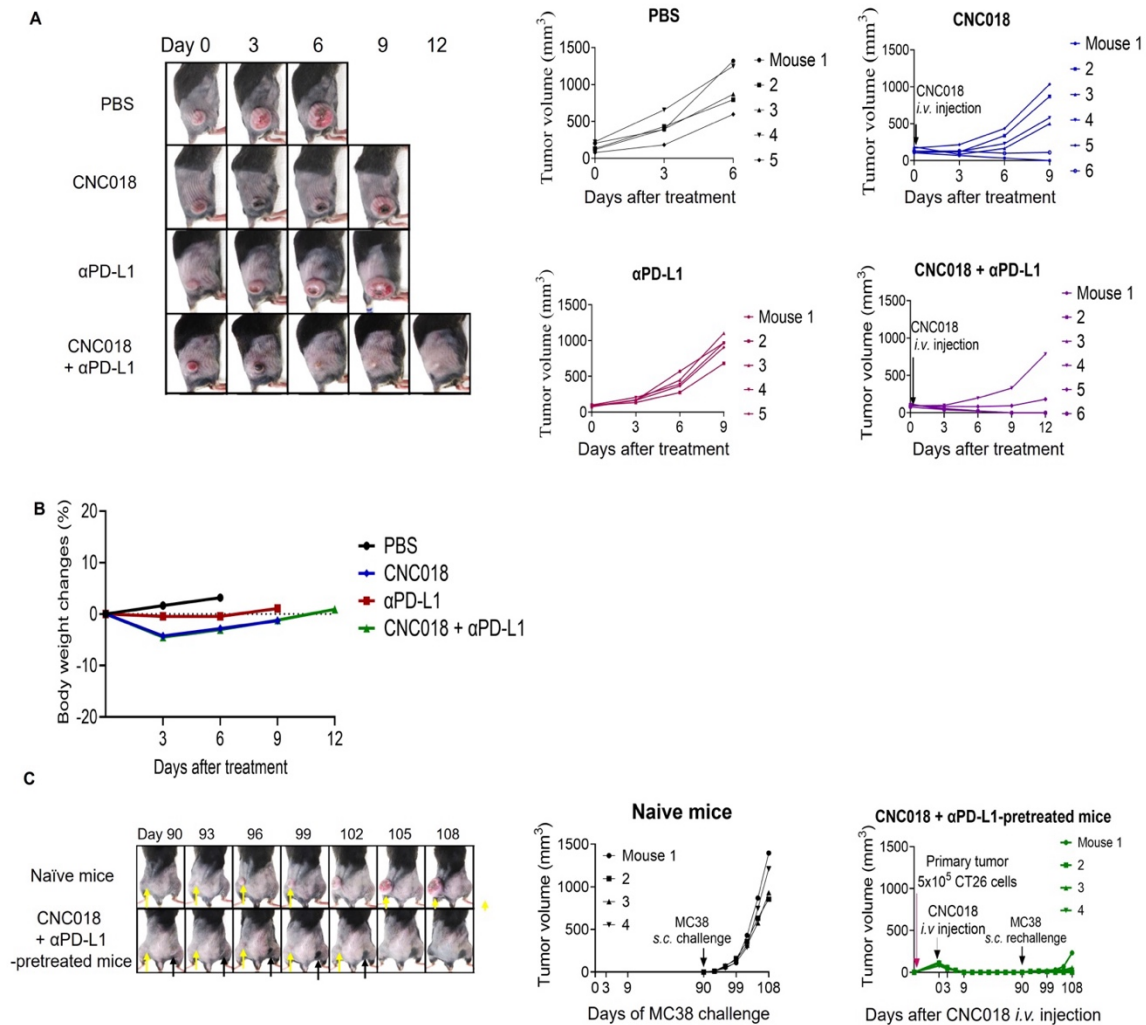


Figure S22. Tumor suppression by the synergistic combination of CNC018 and α PD-L1 in MC38 tumor-bearing mice (related to Figure 6A-C). C57BL/6 mice were inoculated s.c. with MC38 tumor cells (5×10^5) on the right hind flanks. When tumors reached 100 - 120 mm^3 in volume, mice were injected i.v. with CNC018 (2×10^7 CFU) (day 0). An α PD-L1 antibody was injected i.p. on day -1 (200 $\mu\text{g}/\text{mouse}$, twice weekly for five doses). For tumor rechallenge, cured mice were re-implanted s.c. with MC38 cells (1×10^6) on the contralateral flanks on day 90. Naïve age-matched mice ($n = 4$ mice) were used as rechallenge controls. **(A)** Representative images (left) and individual tumor growth curves (right) of mice treated with PBS, CNC018, α PD-L1, or CNC018 + α PD-L1. **(B)** Body weight changes of mice after treatment. **(C)** Representative images (left) and individual tumor growth curves (right) of rechallenged tumors in naïve and cured mice. Scars of primary tumors and rechallenge sites are marked by black and yellow arrows, respectively.

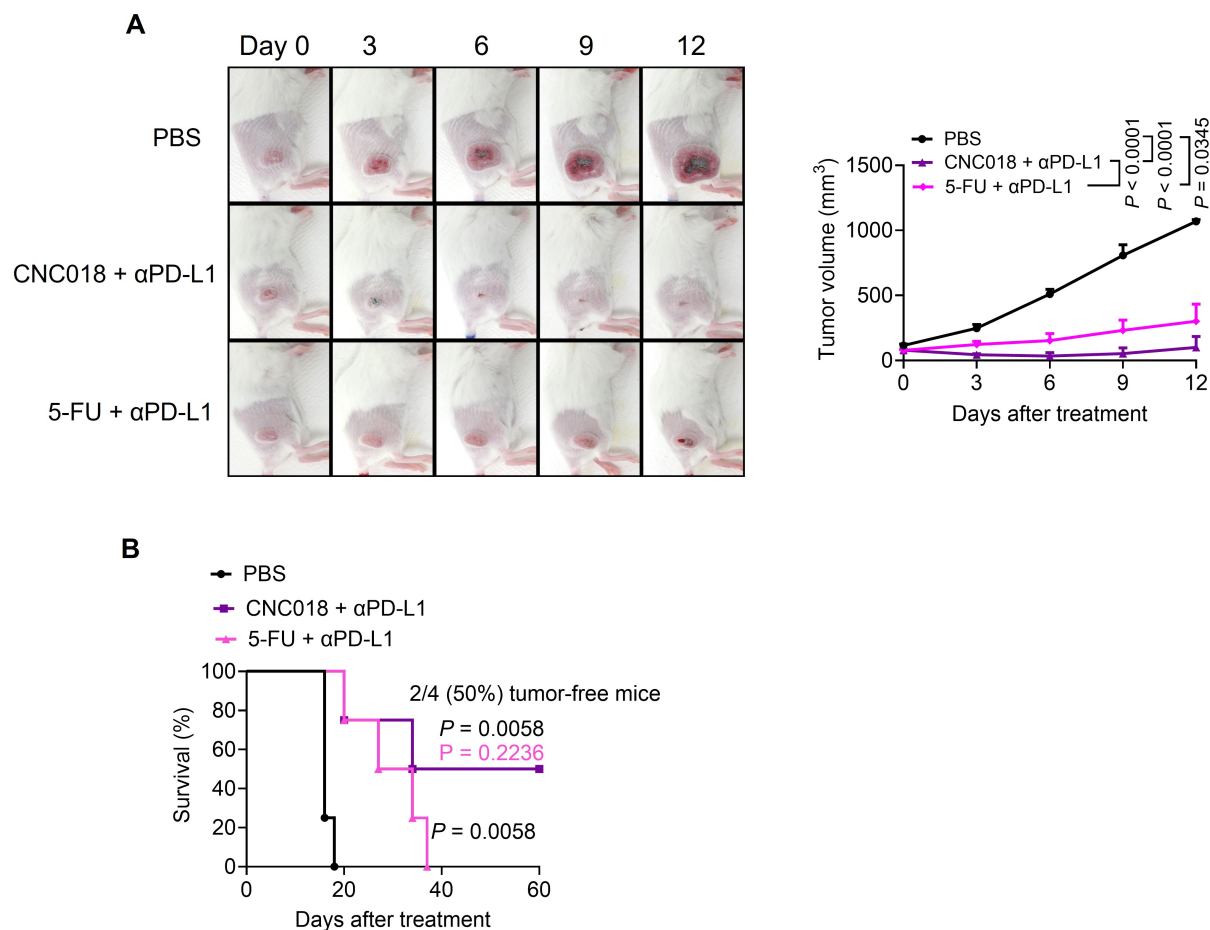


Figure S23. Antitumor effects of 5-FU and CNC018 strain in combination with anti-PD-L1 immunotherapy. BALB/c mice were s.c. implanted with 5×10^5 of CT26 cells. When tumors reached $\sim 100 \text{ mm}^3$ in volume, mice received CNC018 (2×10^7 CFU) or 5-FU (50 mg/kg) and α PD-L1 antibody. CNC018 or 5-FU was i.v. or i.p. injected on day 0, respectively. Anti-PD-L1 (200 $\mu\text{g}/\text{mouse}$, twice weekly schedule for five doses) was i.p. injected starting on day -1. **(A)** Left: representative images of each treated group; Right: average CT26 tumor growth curves ($n = 4$ mice/group; two-way ANOVA with Tukey's multiple comparisons test). **(B)** Kaplan-Meier survival curves of mice from (A) [$n = 4$ mice/group; log-rank (Mantel-Cox) test].

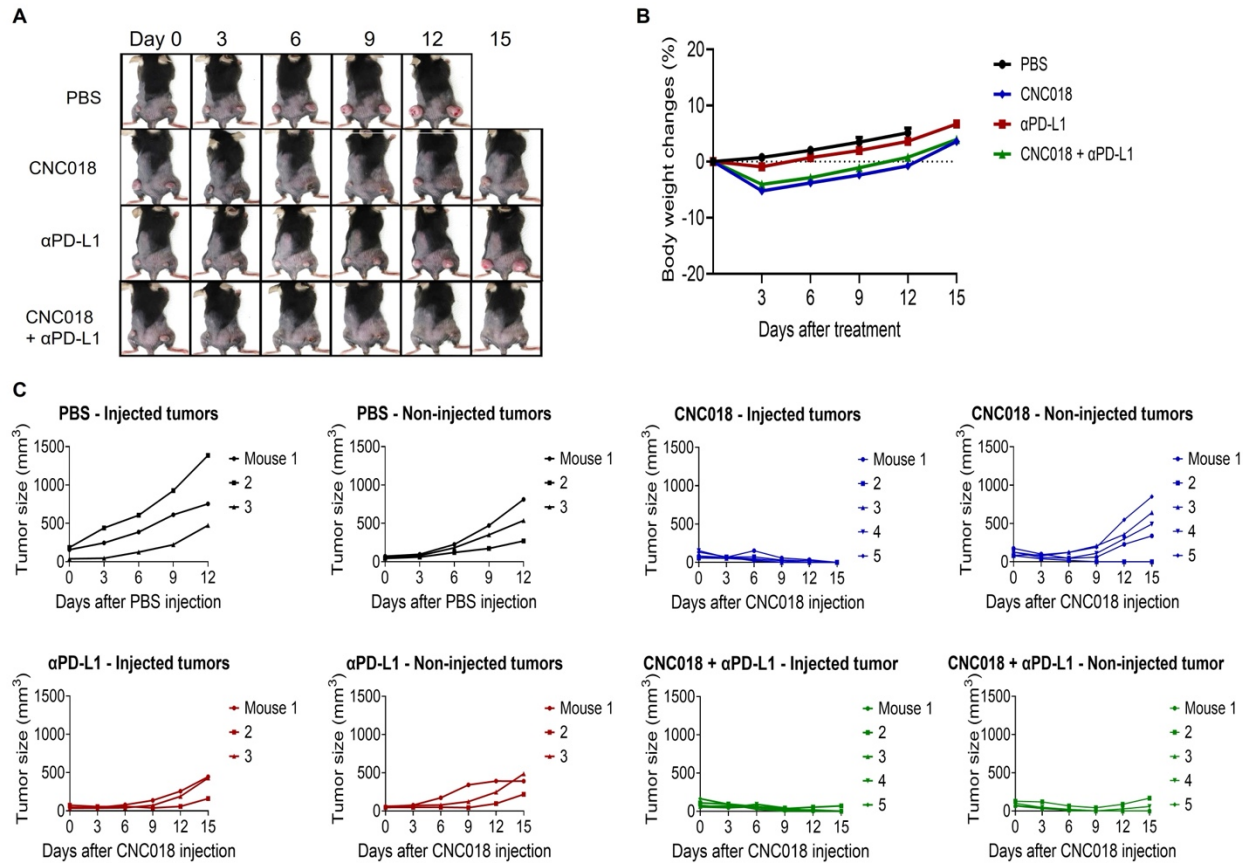


Figure S24. Tumor suppression by the synergistic combination of CNC018 and αPD-L1 in MC38 dual tumor-bearing mice treated by intratumoral injection (related to Figure 6N). MC38 tumor cells (5×10^5) were simultaneously inoculated s.c. into both hind flanks of C57BL/6 mice. When both tumors were 130 - 150 mm³ in volume, mice were intratumorally injected with CNC018 (2×10^7 CFU) into the right tumor (day 0). αPD-L1 antibody (200 μg/mouse) was injected i.p. (day -1, twice weekly for five doses). **(A)** Representative images, **(B)** body weight changes, and **(C)** individual tumor growth curves of bacteria-injected and non-injected tumors are shown.

Table S1. Strains and plasmids are used in this study.

Strains or Plasmids	Descriptions	Sources/Ref.
Bacterial strains <i>S. typhimurium</i>		
14028S	Wild type	ATCC, USA
VNP20009	$\Delta purI$, $\Delta msbB$	ATCC, USA
SHJ2168	$\Delta relA$, $\Delta spoT$ ($\Delta ppGpp$)	[11]
CNC018	$\Delta relA$, $\Delta spoT$, $\Delta SPI-1$, $\Delta SPI-2$	This study
Plasmids		
pKD13	<ul style="list-style-type: none"> - 3.4 kb, KanR flanking FRT sequence, R6K gamma replication origin. - Kanamycin resistance gene template plasmid. 	Gift from Prof. Hyon E. Choy, Chonnam National University, Korea
pKD46	<ul style="list-style-type: none"> - Ampicillin resistance. - Temperature-sensitive replication origin. 	
pCP20	<ul style="list-style-type: none"> - Flipase system. - Ampicillin and chloramphenicol resistance. - Temperature-sensitive replication origin 	

Table S2. Oligonucleotide primers of PCR amplification for bacterial genotyping.

Gene	Primer	Primer name*	Sequence	Expected size (bp)
<i>relA</i>	1	m_wtS_relA-F	AATTTCAATTTGATCACCCATCTGCAAC TGA	715
		m_wtS_relA-R	CGAACATTACATCGAAGAGTTTGTGG AC	
<i>SpoT</i>	2	m_wtS-spoT-F	ATTGCTGAAGGTCGTCGTTAATCACA	2185
		m_wtS-spoT-R	GCATATACGCGCATAACGTTTTGGATTC	
<i>SPI-1</i>	3	m_wtS-SPI1-spaO-F	GGGTGGAAAATGCCAGTAAGGCAATTA ATGA	990
		m_wtS-SPI1-spaO-R	AGCAACAGCACAGACAGCAAT	
<i>SPI-2</i>	4	m_wtS-SPI2-sseF-F	GGTTGATACTCTTATTGCTTAAATAACA GAACGAA	843
		m_wtS-SPI2-sseF-R	CTGAGCATTGTTGGCTAACAGGTTTCAT	

*F, forward primer; R, reverse primer

relA, *spoT*: Bifunctional (p)ppGpp synthase/hydrolase (ppGpp synthesis/degradation)

spaO: Surface presentation of antigens protein (belongs to SPI-1 locus)

sseF: Secretion system effector (belongs to SPI-2 locus)

Table S3. Antibodies used in this study.

Ab ID	Ab description	Manufacturer/Cat. No	Application
Anti-HMGB1 antibody – ChIP Grade	Rabbit Polyclonal Ab	Abcam/ab18256	Western blotting
Goat Anti-Rabbit IgG H&L (HRP)	Polyclonal Ab	Abcam/ab205718	
IL-1 β Mouse ELISA Kit	Specific monoclonal Ab	Thermo Fisher Scientific / BMS6002	Elisa
IFN- γ mouse ELISA Kit	Specific monoclonal Ab	Thermo Fisher/BMS606-2	
TNF alpha Mouse ELISA Kit	Specific monoclonal Ab	Thermo Fisher/BMS607HS	
ATP Assay Kit (Colorimetric/Fluorometric)		Abcam/ab83355	
Nitric Oxide, detection kit		Enzo/ADI-917-202	
Calreticulin (D3E6) XP® Rabbit mAb (PE Conjugate)	Specific monoclonal Ab	Cell Signalling/19780S	Flow cytometry
Rabbit (DA1E) mAb IgG XP® Isotype Control (PE Conjugate)	Specific monoclonal Ab	Cell Signalling/5742S	
PE anti-mouse CD274 (B7-H1, PD-L1) Ab	Specific monoclonal Ab	Biolegend/124308	
PE Mouse IgG2b, κ Isotype Ctrl Antibody	Specific monoclonal Ab	Biolegend/400312	

PE Rat IgG2a, κ Isotype Ctrl Antibody	Specific monoclonal Ab	BioLegend/400508
PE Mouse IgG1, κ Isotype Ctrl Antibody	Specific monoclonal Ab	BioLegend/400112
PE anti-mouse Ki-67 Antibody	Specific monoclonal Ab	BioLegend/652403
Mouse IgG1 APC-conjugated Antibody	Specific monoclonal Ab	Biotechne/400312
Pacific Blue anti-mouse CD45.2 antibody	Specific monoclonal Ab	BioLegend/109820
Anti-mouse CD16/32	TruStain FcX™ Fc blocking solution	BioLegend/101320
Live/dead Fixable aqua dead cell stain kit		Invitrogen/L34957
Anti-mouse CD3-FITC	Clone 17A2	eBioscience/11-0032-82
Anti-mouse CD11c-FITC	Clone N418	eBioscience/11-0114-82
Anti-mouse 11b-FITC	Clone M1/70	BioLegend/101205
Anti-mouse CD4-APC	Clone GK1.5	BioLegend/100412
Anti-mouse CD8a-PE	Clone 53-6.7	eBioscience/12-0081-82
Anti-mouse CD274-PE	Clone 10F.9G2	BioLegend/12-0081-82

Anti-mouse F4/80-PE	Clone BM8	eBioscience/124801-82
Anti-mouse IL-1 β PE	Clone CRM56	eBioscience/12-7018-82
Anti-mouse CD86-PE	Clone GL1	eBioscience/12-0862-82
Anti-mouse CD49b-PE	Clone DX5	BioLegend/108908
FOXP3 Monoclonal Antibody (FJK-16s)-PE	Clone FJK-16S	Ebioscience/12577383
Anti-mouse FOXP3-APC	Clone FJK-16s	eBioscience/77-5775-40
Anti-mouse CD49b-APC	Clone DX5	BioLegend/108909
Anti-mouse CD4-APC	Clone GK1.5	BioLegend/100412
Anti-mouse Gr-1-APC	Clone 1A8	BioLegend/127614
Anti-mouse CD274-APC	Clone B7-H1	BioLegend/124312
Anti-mouse CD206-APC	Clone B7-H1	BioLegend/C068C2
Anti-mouse CD25-PerCP-Cy5.5	Clone PC61	BioLegend/102030
Anti-mouse CD279-PerCP-Cy5.5	Clone RMP130	BioLegend/109120
Anti-mouse granzyme B-PerCP-Cy5.5	Clone QA16A02	BioLegend/372212
Anti-mouse CD8-PerCP-Cy5.5	Clone 53-6.7	BioLegend/100733
Anti-mouse CD62L-PerCP-Cy5.5	Clone MEL-14	BioLegend/104432

FITC anti-mouse/human CD44 Antibody	Clone IM7	BioLegend/103006
Anti-mouse MHCII-PerCP-Cy5.5	Clone M5/114.15.2	BioLegend/107625
Anti-mouse Ly-6G-PerCP-Cy5.5	Clone RB6-8C5	BioLegend/127615
Anti-mouse F4/80-PerCP-Cy5.5	Clone BM8	BioLegend/123128
Anti-mouse Ki-67-PE-Cy7	Clone SolA15	Thermo Fisher Scientific/25469882
PE/Cy7 anti-mouse CD152	Clone UC10-4B9	BioLegend/106313
Anti-mouse CD8 PE-Cy7	Clone 53-6.7	eBioscience/25-0081-82
Anti-mouse CD206 PE-Cy7	Clone C068C2	BioLegend/141719
Anti-mouse CD11c PE-Cy7	Clone N418	Thermo Fisher Scientific/25-0114-82
Anti-mouse CTLA-4 PE-Cy7	Clone UC10-4B9	BioLegend/106313
Anti-mouse PD-L1 PE-Cy7	Clone B7-H1	EbioScience/25598342
Anti-mouse IFN γ -APC-Cy7	Clone XMG1.2	BioLegend/505849
Anti-mouse PD-1-APC-Cy7	Clone 29F.1A12	BioLegend/135224
Anti-mouse CD44-APC-Cy7	Clone IM7	BioLegend/103028
Anti-mouse CD86-APC-Cy7	Clone GL-1	BioLegend/105029
PE anti-mouse TCR β chain Antibody	Clone H57-597	BioLegend/109208

PE anti-mouse CD170 (Siglec-F) Antibody	Clone S17007L	Biolegend/155506	
APC/Cyanine 7 anti-mouse CD16 Antibody	Clone S17014E	Biolegend/158014	
PE/Cyanine7 anti-mouse CD54 Antibody	Clone YN1.1.7.4	Biolegend/116122	
H-2Ld MuLV gp70 Tetramer-SPSYVYHQF-APC	Clone 53-6.7	MBL/TM-M521-1	
Anti-HMGB1, ChIP grade	Polyclonal Ab	Abcam	HMGB1 Western blotting
rabbit anti-CALR antibody	Polyclonal Ab	Abcam	CALR Western blotting
InVivoMAb anti-mouse IFN γ	XMG1.2	Bioxcell/BE0055	IFN- γ neutralizing
HMGB1 Neutralizing antibody [SQab20175]	Polyclonal Ab	Arigo/ARG66714	HMGB1 neutralization
InVivoMAb anti-mouse PD-L1 (B7-H1)	Clone 10F.9G2	Bio X Cell/BE0101	PD-L1 neutralization

<i>InVivo</i> MAB rat IgG2b isotype control	Clone LTF-2	Bio X Cell/BE0090	PD-L1 neutralization control
<i>InVivo</i> MAB anti-mouse PD-1 (CD279)	Clone RMP1-14	Bio X Cell/BE0146	PD-1 neutralization
<i>InVivo</i> MAB rat IgG2a isotype control, anti-trinitrophenol	Clone 2A3	Bio X Cell/BE0089	PD-1 neutralization control
<i>InVivo</i> MAB anti-mouse CTLA-4 (CD152)	Clone 9H10	Bio X Cell/BE0131	CTLA-4 neutralization
<i>InVivo</i> MAB polyclonal Syrian hamster IgG	Clone polyclonal	Bio X Cell/BE0087	CTLA-4 neutralization control
Anti-mouse CD8 α	Clone 2.43	Bio X Cell/BP0061	CD8 ⁺ T depletion
Rat IgG2b isotype control Ab	Clone LTF-1	Bio X Cell/BP0090	T-cell depletion control
CD3 ϵ MicroBead Kit, mouse		Miltenyi Biotec/130-094-973	Harvesting CD3 ⁺ T cells
LS columns		Miltenyi Biotec/130-042-401	Harvesting CD3 ⁺ T cells

Table S4. Xenograft pathological subtype changes of patient colon cancer.

Patient ID	Age	Gender	Histocompatibility						
			Cancer	Stroma	Tumor necrosis	Extracellular mucus in tumors	Inflammatory response around the tumor	Intratumor interstitial fibrosis	Control normal tissue in the slide
NM-P-C-6	61	Female	70%	30%	Yes, 5%	Yes, 10%	Intermediate	60%	No

Table S5. CDI value of CNC018 plus ICB blockade in CT26 and MC38 tumor models.

Average tumor volume (mm ³)	Control (PBS)	A (CNC018)	B (α PD-L1)	AB (CNC018 + α PD-L1)	CDI	Interpretation
CT26 tumor volume (day 12)	1033.4	515.8	564.8	37.74	0.13	Significant synergism
MC38 tumor volume (day 9)	1629	925.6	597.8	85.2	0.25	Significant synergism
Average tumor volume (mm ³)	Control (PBS)	A (CNC018)	B (α CTLA-4)	AB (CNC018 + α CTLA-4)	CDI	Interpretation
CT26 tumor volume (day 12)	1033.4	515.8	252.1	0	0	Significant synergism
Average tumor volume (mm ³)	Control (PBS)	A (CNC018)	B (α PD-1)	AB (CNC018 + α PD-1)	CDI	Interpretation
CT26 tumor volume (day 12)	1033.4	515.8	758.7	301.8	0.80	Synergism

CDI, coefficient of drug interaction; $CDI = (AB/control)/[(A/control) \times (B/control)]$.